

# Ferromagnetic Exchange in Bichloride Bridged Cu(II) Chains: Magnetostructural correlations between ordered and disordered systems

Susan N. Herringer,<sup>1</sup> Christopher P. Landee,<sup>2</sup> Mark M. Turnbull\*,<sup>1</sup> Jordi Ribas-Ariño\*,<sup>3</sup> Juan J. Novoa,<sup>3</sup> Matthew Polson<sup>4</sup> and Jan L. Wikaira<sup>4</sup>

<sup>1</sup> Carlson School of Chemistry and Biochemistry, Clark University, 950 Main St. Worcester, MA 01610, USA

<sup>2</sup> Dept. of Physics, Clark University, 950 Main St. Worcester, MA 01610, USA

<sup>3</sup> Departament de Ciència de Materials i Química Física & IQTCUB, Facultat de Química, Universitat de Barcelona, Martí i Franquès 1, 08028-Barcelona, Spain

<sup>4</sup> Dept. of Chemistry, University of Canterbury, Private Bag 4800, Christchurch, New Zealand

*email: mturnbull@clarku.edu*

## ABSTRACT

The synthesis, structure, magnetic properties and theoretical analysis of a new phase of dichloro(2-chloro-3-methylpyridine)copper(II) (**2**), and its isomorphous analogue dichloro(2-bromo-3-methylpyridine)copper(II) (**3**) are reported. Both complexes crystallize in the orthorhombic space group *Pbca* and present square pyramidal Cu(II) ions bridged into chains by chloride ions with each copper(II) bearing a single pyridine ligand. Variable temperature magnetic susceptibility measurements were well fit by a uniform 1D-ferromagnetic chain model with: **2**,  $J = 69.0(7)$  K,  $C = 0.487$  emu-K/mole-Oe; **3**,  $J = 73.9(4)$  K,  $C = 0.463$  emu-K/mol-Oe ( $H = -J\sum_i S_i \cdot S_j$  Hamiltonian). The experimental *J*-values were confirmed via theoretical calculations. Comparison to a known disordered polymorph of dichloro(2-chloro-3-methylpyridine)copper(II), **1**, shows marked differences as there are significant antiferromagnetic next-nearest neighbor interactions in **1** in addition to randomness induced by the disorder with provide a distinctly different magnetic response. The differences in magnetic behavior are attributed principally to the structural difference in the Cu(II) coordination sphere, **1** being significantly closer to trigonal-bipyramidal, which difference changes both the nearest and next-nearest neighbor interactions.

## INTRODUCTION

The structure and magnetic behavior of bihalide bridged Cu(II) chains have been studied for decades. One common structural motif in these complexes exhibits two trans halide ions and two trans ancillary ligands (frequently amines) coordinated to the copper ion in a pseudosquare planar array. These molecules are then linked into roughly linear chains by pairs of short Cu $\cdots$ X contacts ( $\sim 2.5\text{--}3$  Å) between the molecules. Cu(py) $_2$ X $_2$  complexes are prototypical<sup>(1)</sup> of these structures, but a wide variety of substituted pyridine complexes,<sup>(2)</sup> as well as other heterocyclic amines,<sup>(3)</sup> are well-known in such complexes with both CuCl $_2$  and CuBr $_2$ . With chelating ligands, the cis-substituted CuL $_2$ X $_2$  compounds are formed in which case the bridging halide ions generate quasi-helical structures which still maintain the bihalide-bridging motif.<sup>(4)</sup> Although magnetic behavior has not been determined for all of these compounds, those where such interactions have been reported share the common theme that the interactions via the bihalide bridge are antiferromagnetic, regardless of the cis/trans nature of the primary coordination at the Cu(II) center.

The same is not true for five-coordinate, bihalide-bridged Cu(II) chains and oligomers. A somewhat smaller number of these compounds have been structurally characterized, and they fall into two classes: those where the ancillary ligand (nonbridging) is also an ion (frequently another halide ion) and those where the ancillary ligand is a neutral species. In the former category are several ammonium salts such as (4-benzylpiperidinium)CuCl $_3$ ,<sup>(5)</sup> (dimethylammonium)CuCl $_3$ ,<sup>(6)</sup> (*N*-methyl-*N*-butylimidazolium)CuCl $_3$ ,<sup>(7)</sup> (ethyltrimethylammonium)CuCl $_3$ ,<sup>(8)</sup> and (diethyldimethylammonium)CuCl $_3$ ,<sup>(9)</sup> as well as the (tetramethylammonium)CuCl $_3$  compound<sup>(10)</sup> which exhibits a trichloride bridge between Cu(II) ions. Among these complexes, both ferromagnetic and antiferromagnetic interactions have been observed via the bridging chloride ions.

There are very few compounds in the latter category where the ancillary ligand is neutral. Dichlorodimethylnitrosaminecopper(II),<sup>(11)</sup> dichlorotetramethylenesulfoxidecopper(II),<sup>(12)</sup> and dichlorodimethyl sulfoxidecopper(II)<sup>(12)</sup> are all uniform bichloride bridged chains with an O-bound ligand occupying the fifth coordination site (in the latter two compounds, short O $\cdots$ Cu distances provide a potential third bridge). Dichloro(1,4-oxathiane)copper(II) generates bichloride bridged chains, but with two different Cu(II) sites in the chain in an AABAAB pattern.<sup>(13)</sup> The A-site is a five-coordinate CuCl $_4$ O moiety (with the O from an oxathiane), while the B-site is tetragonal, CuCl $_4$ S $_2$ , with a square planar array of chloride ions and semicoordinate S atoms (from oxathiane molecules in adjacent chains) occupying the axial positions. The 2-allyltetrazole copper chloride complex<sup>(14)</sup> is similar to the A-sites having a CuCl $_4$ N coordination sphere and the B-sites having a CuCl $_4$ N $_2$  coordination sphere. Of these, only the copper-sulfoxide complexes have been examined for their magnetic behavior, and both compounds showed dominant ferromagnetic exchange within the chains.

We recently reported the synthesis, structure, and magnetic behavior of a new member of this unusual class of pentacoordinate Cu(II) coordination polymers, the complex *catena*-dichloro(2-chloro-3-methylpyridine)copper(II) (**1**).<sup>(15)</sup> Due to its crystallographic disorder, it provided a random-exchange ferromagnetic chain which exhibited magnetic frustration due to next-nearest neighbor interactions. Both experimental and theoretical analysis of its magnetic behavior (see Figure 1) has been previously reported.<sup>(15)</sup> The bulk magnetic behavior of the complex was justified as a result of competing interactions within the chain structure through the theoretical calculations. Three structurally and magnetically distinct nearest-neighbor interactions occur, as a result of the structural disorder, which provide three equally distinct ferromagnetic exchange pathways, while the corresponding next-nearest-neighbor interactions are all antiferromagnetic (but of similar magnitude to each other).

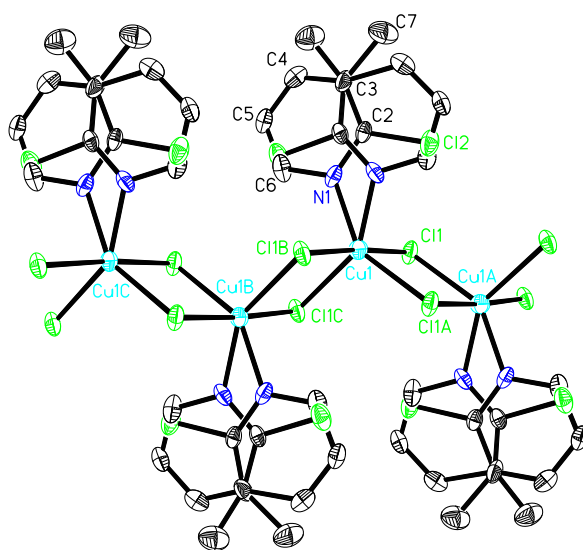


Figure 1. Thermal ellipsoid plot (50% probability) of a portion of one chain of *catena*-dichloro(2-chloro-3-methylpyridine)copper(II), **1**. The pyridine ligands are disordered (50:50 occupancy) and both positions are shown at each Cu(II) ion. Hydrogen atoms have been removed for clarity.

Further evidence to support the analysis of the compounds' magnetic behavior can be provided through comparison with structurally similar complexes that lack the disorder observed previously, and we have isolated two related compounds, one of which is an ordered polymorph of **1**. Here we report the synthesis, structure, magnetic properties, and theoretical analysis of that second phase of dichloro(2-chloro-3-methylpyridine)copper(II) (**2**) and its isomorphous analogue dichloro(2-bromo-3-methylpyridine)copper(II) (**3**).

## EXPERIMENTAL

2-Chloro-3-methylpyridine, 2-bromo-3-methylpyridine, and 1-propanol were purchased from Aldrich Chemical Co.. Copper chloride was obtained from J.T. Baker. All chemicals were used as received. IR spectra were recorded on a PerkinElmer FTIR: Paragon 500. X-band EPR was carried out on a Bruker EMX EPR spectrometer at room temperature. Elemental analyses were carried out by Marine Science Institute, University of California, Santa Barbara CA 93106.

### *catena*-(2-Chloro-3-methylpyridine)dichlorocopper(II) Phase A (**1**)<sup>(16)</sup>

CuCl<sub>2</sub>·2H<sub>2</sub>O (0.258 g, 1.51 mmol, 50% excess) was dissolved in 4.0 mL of 1-propanol with warming. 2-Chloro-3-methylpyridine (0.128 g, 1.00 mmol) was dissolved in 2.0 mL of 1-propanol and warmed. The CuCl<sub>2</sub> solution was added to the pyridine solution slowly with stirring and a green solution resulted. The solution was covered with a watch glass and allowed to cool to room temperature slowly. Acicular clusters of yellow crystals formed after 2 days. The mixture was filtered, and the crystals were washed with cold 1-propanol and allowed to air-dry to give 0.085g (32.4%). IR (KBr):  $\nu$  3079w, 3015w, 1588s, 1577m, 1440m, 1399s, 1275w, 1233m, 1208m, 1191w, 1136w, 1109s, 1070m, 1033w, 998w, 837w, 802s, 728m, 707s, 570w, 518w, 459w cm<sup>-1</sup>. Anal. Calc. (found) for C<sub>6</sub>H<sub>6</sub>NCl<sub>3</sub>Cu: C, 27.50(27.15); H, 2.31(2.32); N, 5.35(5.22)%.

### *catena*-(2-Chloro-3-methylpyridine)dichlorocopper(II) Phase B (**2**)

CuCl<sub>2</sub>·2H<sub>2</sub>O (0.254 g, 1.49 mmol, 50% excess) was dissolved in 3 mL of 1-propanol with warming. 2-Chloro-3-methylpyridine (0.134 g, 1.05 mmol) was dissolved in 2 mL of 1-propanol and warmed. The CuCl<sub>2</sub> solution was added to the pyridine solution slowly with stirring. The solution was allowed to cool to room temperature. The green solution was covered with parafilm with a few holes poked through and then placed in a cold room (~5 °C). Amber crystals started to form after 1 h. After 2 days, yellow (compound **1**) and amber crystals were both present. The solution was warmed gently until the yellow crystals dissolved and the solution was allowed to continue to crystallize at ~5 °C. Amber crystals were harvested by suction filtration after 3 weeks, which were washed with cold 1-propanol and allowed to air-dry to give 0.178 g (67.9%). IR (KBr):  $\nu$  3089w 3055w, 3011w, 2967w, 1590m, 1574m, 1455m, 1444s, 1400s, 1387m, 1284w, 1236w, 1212m, 1199m, 1137w, 1110s, 1070m, 1052w, 1006w, 839w, 800s, 730m, 705s, 573w cm<sup>-1</sup>. Anal. Calc. (found) for C<sub>6</sub>H<sub>6</sub>NCl<sub>3</sub>Cu: C, 27.50 (27.4); H, 2.31(2.41); N, 5.35(5.30)%.

### *catena*-(2-Bromo-3-methylpyridine)dichlorocopper(II) (**3**)

CuCl<sub>2</sub>·2H<sub>2</sub>O (0.259 g, 1.52 mmol, 50% excess) was dissolved in 5 mL of 1-propanol with warming. 2-Bromo-3-methylpyridine (0.174 g, 1.01 mmol) was dissolved in 2 mL of 1-propanol and warmed. The CuCl<sub>2</sub> solution was added to the pyridine solution slowly with stirring. The resulting solution was allowed to cool to room temperature slowly and covered with a watch glass. After 2 days, blue crystals of (2-bromo-3-methylpyridine)<sub>2</sub>CuBr<sub>2</sub> had formed;<sup>(17)</sup> the crystals were dissolved back into solution with 0.5 mL of 1-propanol and warming [Note: the presence of excess copper(II) in the solution reduces, but does not eliminate the initial formation of the bis-complex. However, it redissolves easily and does not contaminate the final product]. The solution was allowed to slowly return to room temperature. Amber crystals formed within 24 h. The crystals were recovered by suction filtration, washed with cold 1-propanol, and allowed to air-dry to give 0.210 g (68.5%). IR (KBr):  $\nu$  3085w, 3048w, 1586m, 1571m, 1457m, 1444m, 1434m, 1395s, 1278w, 1233w, 1207m, 1192w, 1128m, 1096s, 1060m, 1049w, 1004m, 831w, 801s, 723m, 689m cm<sup>-1</sup>. Anal. Calc. (found) for C<sub>6</sub>H<sub>6</sub>NCl<sub>2</sub>CuBr: C, 23.51(23.4); H, 1.97(1.80); N, 4.57 (4.58)%.

### X-ray Determination

Data collections were carried out on a Siemens P4 diffractometer utilizing Mo-K $\alpha$  radiation ( $\lambda = 0.71073$ ) and a graphite monochromator. The data collection, cell refinement, and data reduction were performed using SHELXTL.<sup>(18)</sup> Absorption corrections were made from redundant data using SADABS.<sup>(19)</sup> A preliminary report of the structure of **1** has been published.<sup>(15)</sup> The structures of **2** and **3** were solved employing direct methods and expanded by Fourier techniques.<sup>(20)</sup> Non-hydrogen atoms were refined anisotropically. Hydrogen atoms were placed in calculated positions and refined using a riding model with fixed isotropic *U* values. Full crystal and refinement details for **1–3** are given in Table 1 while selected bond lengths and angles are given in Table 2. Crystallographic data from single crystal refinements of **1–3** were used for comparison to powder X-ray diffraction data to establish the phase and purity of the samples used for magnetic studies. The structures have been deposited with the CCDC (**1**, #843602; **2**, #1006829; **3** #1006828). These data can be obtained free of charge from The Cambridge Crystallographic Data Centre via [www.ccdc.cam.ac.uk/data\\_request/cif](http://www.ccdc.cam.ac.uk/data_request/cif).

### Magnetic Susceptibility

Magnetic data were collected using a Quantum Design MPMS-XL SQUID magnetometer. The powdered samples used in the magnetic studies were prepared from crushed single crystals. Samples were placed in gelatin capsules, and the magnetic moments were measured using magnetic fields of 0–50 kOe at 1.8 K. Several data points were collected as the magnetic field was brought back to 0 kOe to check for hysteresis effects; none were observed. The data are shown in the Supporting Information as Figure S1 (**2**) and Figure S2 (**3**). Temperature dependent magnetic

susceptibility data were collected over a temperature range of 1.8–310 K in an applied magnetic field of 1 kOe. Background corrections were measured using an empty gelatin capsule. Temperature independent diamagnetic corrections (DIA), calculated from Pascal's constants,<sup>(21)</sup> and the temperature independent paramagnetism (TIP) correction for copper,  $60 \times 10^{-6} \text{ cm}^3 \text{ mol}^{-1}$ , were applied to the data sets.

### Computational Details

Following the same procedure described in ref 15, the values of the magnetic interactions ( $J$ ) between the  $S = 1/2$  spin centers were evaluated by means of density functional theory (DFT) calculations conducted with the Gaussian 09 program<sup>(22)</sup> using the B3LYP functional<sup>(23)</sup> and an Ahlrichs TZVP basis set<sup>(24)</sup> on all atoms. The  $J$  values for each cluster model were obtained by solving a set of equations involving the energies of properly chosen spin states, as described in ref 25.

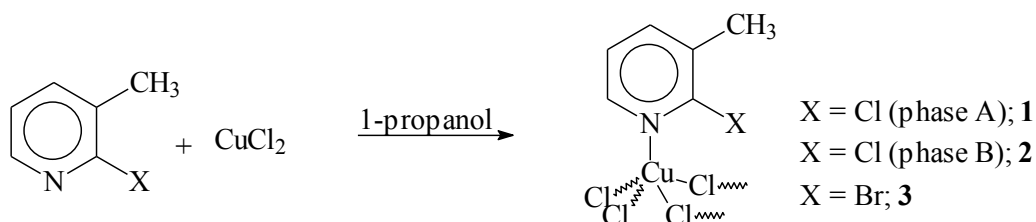
Table 1 – X-Ray data collection and refinement parameters for compounds **1-3**.

Compound	1	2	3
Empirical formula	C <sub>6</sub> H <sub>6</sub> NCl <sub>3</sub> Cu	C <sub>6</sub> H <sub>6</sub> NCl <sub>3</sub> Cu	C <sub>6</sub> H <sub>6</sub> NCl <sub>2</sub> CuBr
Formula weight	262.01	262.01	
Temperature	108(2) K	111(2) K	111(2) K
Wavelength	0.71073 Å	0.71073 Å	0.71073 Å
Crystal system (space group)	Monoclinic ( <i>C2/c</i> )	Orthorhombic ( <i>Pbca</i> )	Orthorhombic ( <i>Pbca</i> )
Unit cell: (Å)			
a	10.0735(5)	16.0831(4)	16.3043(4)
b (Å)	15.3951(8)	12.2128(3)	12.2138(3)
c (Å)	6.2152(8)	18.5204(5)	18.5935(5)
$\alpha$ (°)	90	90	90
$\beta$ (°)	111.293(2)	90	90
$\gamma$ (°)	90	90	90
Volume (Å <sup>3</sup> )	898.07(13)	3637.77(16)	3702.66(16)
Z	2	8	8
Density (calculated)	1.938 Mg/m <sup>3</sup>	1.914 Mg/m <sup>3</sup>	2.199 Mg/m <sup>3</sup>
Absorption coefficient	3.254 mm <sup>-1</sup>	3.214 mm <sup>-1</sup>	7.185 mm <sup>-1</sup>
F(000)	516	2064	2352
Crystal size (mm <sup>3</sup> )	0.31 x 0.05 x 0.03	0.40 x 0.36 x 0.32	0.45 x 0.34 x 0.10
Theta range for data collection	2.54 to 60.63°	2.20 to 27.53°	2.52 to 30.51°
Index ranges	-14 ≤ h ≤ 14	-20 ≤ h ≤ 20	-23 ≤ h ≤ 23

	$-21 \leq k \leq 22$	$-15 \leq k \leq 15$	$-17 \leq k \leq 16$
	$-8 \leq l \leq 8$	$-24 \leq l \leq 24$	$-26 \leq l \leq 26$
Reflections collected ( $R_{\text{int}}$ )	10918	86912	62535
Independent reflections	1381 (0.0608)	4179 (0.0374)	5610 (0.0752)
Completeness to theta	99.40%	99.80%	99.30%
Absorption correction	Semi-empirical		
Refinement method	Full-matrix least-squares on F2		
Data / restraints / parameters	1381 / 9 / 105	4179 / 0 / 201	5610 / 0 / 201
Goodness-of-fit on F2	1.238	1.141	1.014
Final indices $R_1(wR_2)$ ; [ $I > 2\sigma(I)$ ]	0.0548 (0.1109)	0.0164 (0.0411)	0.0309 (0.0669)
Final indices $R_1(wR_2)$ ; all data	0.0825 (0.1210)	0.0193 (0.0480)	0.0632 (0.0759)
Max. diff. peak (hole) ( $e/\text{\AA}^3$ )	1.043 (-1.473)	0.441 (-0.370)	1.833 (-0.858)

## RESULTS and DISCUSSION

Reaction of 2-halo-3-methylpyridine with excess copper(II) chloride in 1-propanol gave the products (2-halo-3-methylpyridine)dichlorocopper(II) (**1–3**) in 30–70% yield (Scheme 1).



**Scheme 1** – Preparation of **1-3**.

Compound **1** occurs as yellow, acicular clusters, while **2** and **3** form amber, rod-shaped crystals. Compounds **1** and **2** form as the kinetic and thermodynamic products of the crystallization, respectively. Compound **1** crystallizes initially from the reaction mixture (1–2 days). However, if the reaction mixture is left to stand, the crystals of **1** slowly dissolve and crystals of **2** form over the course of several days. The formation of **2** can be hastened by warming the mixture to redissolve compound **1** after it has formed. All three compounds were analyzed by single-crystal X-ray diffraction. Data collection and refinement parameters are given in Table 1.

## X-ray Structure of Catena-(2-chloro-3-methylpyridine)dichlorocopper(II) (**2**)

The asymmetric unit of compound **2** is shown in Figure 2; selected bond lengths and angles are given in Table 2. Compound **2** crystallizes in the orthorhombic space group *Pbca* with two crystallographically independent copper ions within the asymmetric unit, both of which are five-coordinate. Bond lengths and angles within the pyridine ring are comparable to those found in the complexes  $\text{Cu}(\text{2-Cl-3-Mepy})_2\text{X}_2$ .<sup>(17)</sup> The pyridine rings are nearly planar with a mean deviation of the constituent atoms of 0.0037 and 0.0043 Å for the N1 and N11 rings, respectively. The chlorine and methyl substituents are almost coplanar with the pyridine rings, deviating 0.0131/0.0012 Å and 0.0054/0.0321 Å, respectively, for the N1 and N11 rings. Each of the pyridine rings occupies an equatorial position of their respective copper coordination spheres.

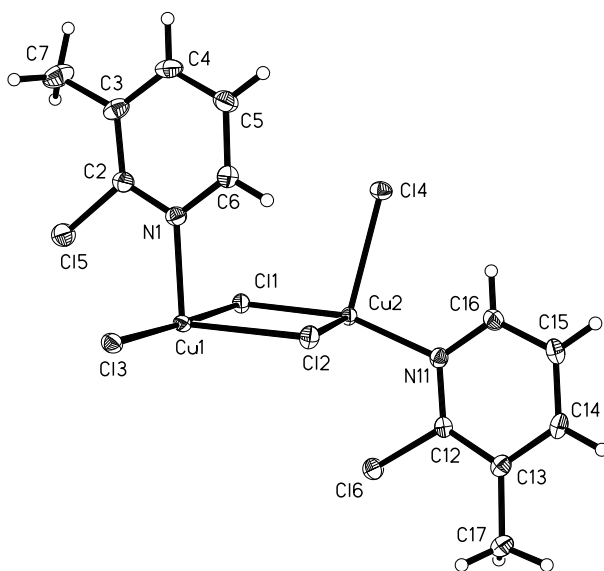


Figure 2: The asymmetric unit of **2** showing 50% probability ellipsoids for refined atoms. Only atoms whose positions were refined are labeled.

The five-coordinate copper(II) chains of **2** form parallel to the *b*-axis (Figure 3) via bridging chloride ions. Using the continuous symmetry measure (CSM) approach,<sup>(26)</sup> the two copper coordination spheres can be shown to be significantly closer to square pyramidal [ $S(C_{4v}) = 0.929$  and  $1.03$ ] than trigonal bipyramidal [ $S(D_{3h}) = 3.65$  and  $4.46$ ] for each Cu1 and Cu2, respectively. There are eight independent Cu–Cl bonds, which vary in length from 2.2698(4) Å to 2.5581(4) Å. The Cu1–Cl–Cu2 angles range from 90.171(15)° to 95.399(15)°. There exist two types of bridges between the copper ions: (1) equatorial–equatorial (eq–eq) bridges, where the bridging chloride ion occupies an equatorial position for both Cu1 and Cu2 (Cl11 and Cl13) and (2) axial–equatorial (ax–eq) bridges, where the bridging chloride ion occupies an axial position on one copper ion and an equatorial position on the other copper ion (Cl14 and Cl12). For example, Cl14A is



axial to Cu2A and Cl2 is axial to Cu1. The dihedral angle Cu1–Cl4–Cu2A–Cl2A is  $-172.4^\circ$  while that of Cu2A–Cl4A–Cu1–Cl2 is  $93.7^\circ$ . This second dihedral angle provides a symmetric twist to the chain, occurring alternately clockwise and anticlockwise successively along the chain. The twist prevents the close approach of neighboring chains.

Table 2. Selected bond lengths (Å) and angles ( $^\circ$ ) for **1-3**. Data in bold type refer to structural parameters for the chloride bi-bridged chains.

Bond lengths(Å)	<b>1</b>	<b>2</b>	<b>3</b>
Cu(1)-N(1)	1.967(8)	2.0399(14)	2.036(3)
<b>Cu(1)-Cl(1)</b>	<b>2.2915(10)</b>	<b>2.3400(4)</b>	<b>2.3411(8)</b>
<b>Cu(1)-Cl(1)#1/Cl2</b>	<b>2.4582(12)</b>	<b>2.5581(4)</b>	<b>2.5712(8)</b>
<b>Cu(1)-Cl3/Cl3#2</b>		<b>2.3196(4)</b>	<b>2.3235(8)</b>
<b>Cu1-Cl4/#2</b>		<b>2.2698(4)</b>	<b>2.2723(9)</b>
Cu(2)-N(11)		2.0067(14)	2.004(2)
<b>Cu(2)-Cl(1)</b>		<b>2.3102(4)</b>	<b>2.3108(8)</b>
<b>Cu(2)-Cl(2)</b>		<b>2.2915(4)</b>	<b>2.2942(8)</b>
<b>Cu(2)-Cl(3)</b>		<b>2.3511(4)</b>	<b>2.3495(8)</b>
<b>Cu(2)-Cl4/Cl4#3</b>		<b>2.5524(4)</b>	<b>2.5652(9)</b>
N1-Cu1-Cl1	96.7(2)	88.57(4)	88.67(8)
N1-Cu1-Cl1/Cl2	87.2(2)	95.47(4)	95.00(8)
N1-Cu1-Cl1/Cl3	141.6(2)	90.07(4)	89.91(8)
N1-Cu1-Cl1/Cl4	110.3(2)	162.41(4)	163.25(8)
<b>Cl1-Cu1-Cl2</b>	<b>86.44(4)</b>	<b>83.740(14)</b>	<b>83.64(3)</b>
<b>Cl1-Cu1-Cl3</b>	<b>175.98(8)</b>	<b>177.634(17)</b>	<b>177.46(3)</b>
<b>Cl1-Cu1-Cl4</b>	<b>91.19(5)</b>	<b>90.452(15)</b>	<b>90.52(3)</b>
<b>Cl2-Cu1-Cl3</b>	<b>107.82(7)</b>	<b>98.317(15)</b>	<b>98.59(3)</b>
<b>Cl2-Cu1-Cl4</b>		<b>101.875(16)</b>	<b>101.54(3)</b>
<b>Cl3-Cu1-Cl4</b>		<b>90.267(15)</b>	<b>90.23(3)</b>
<b>N11-Cu2-Cl1</b>		<b>162.73(4)</b>	<b>163.21(8)</b>
<b>N11-Cu2-Cl2</b>		<b>86.14(4)</b>	<b>86.40(8)</b>
<b>N11-Cu2-Cl3</b>		<b>90.13(4)</b>	<b>89.77(8)</b>
<b>N11-Cu2-Cl4</b>		<b>99.72(4)</b>	<b>99.85(8)</b>
<b>Cl1-Cu2-Cl2</b>		<b>90.682(15)</b>	<b>90.83(3)</b>
<b>Cl1-Cu2-Cl3</b>		<b>91.140(15)</b>	<b>91.34(3)</b>
<b>Cl1-Cu2-Cl4</b>		<b>97.529(15)</b>	<b>96.91(3)</b>
<b>Cl2-Cu2-Cl3</b>		<b>173.008(17)</b>	<b>173.52(3)</b>
<b>Cl2-Cu2-Cl4</b>		<b>103.438(15)</b>	<b>102.93(3)</b>
<b>Cl3-Cu2-Cl4</b>		<b>83.011(14)</b>	<b>82.87(3)</b>
<b>Cu1-Cl1-Cu1#1/Cu2</b>	<b>93.56(4)</b>	<b>95.399(15)</b>	<b>95.54(3)</b>

Cu1-Cl2-Cu2		90.171(15)	89.95(3)
Cu1-Cl3-Cu2		95.177(16)	95.45(3)
Cu1-Cl4-Cu2		91.114(15)	91.04(3)

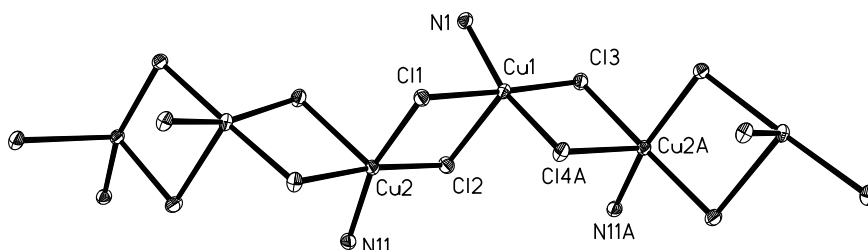


Figure 3: Depiction of the 5-coordinate geometry of the copper ions in chains of **2** and **3** showing only those atoms in the copper coordination spheres for clarity

Compound **2** is similar to other chloride-bridged square pyramidal copper complexes whose geometries can be described as “4 + 1” with four short Cu–Cl bonds and one longer Cu–Cl bond, although in **2** one of the equatorially coordinated atoms is a pyridine nitrogen.<sup>(5-10)</sup> The long Cu–Cl axial bond here, however, is shorter (2.5 Å) than that found in the usual 4 + 1 geometry (~2.7 Å). Typical of this group of five-coordinate copper complexes is the distortion of the two distinctly different *trans* angles in the basal plane; one angle is nearly linear (~180°), while the other *trans* Cl–Cu–Cl angle is considerably bent (~145–160°). Here, the two *trans* Cl–Cu–Cl angles for Cu1 are 177.634(17)/162.41(4)° and 173.008(17)/162.73(4)° for Cu2, both of which are less distorted than typical complexes of “4 + 1” copper chloride coordination polymers. In general, the preferred stereochemistry of five coordinate copper(II) systems is that of a “4 + 1” geometry with a Cu–Cl’ distance in the range of 2.65–2.75 Å and a *trans* angle difference ( $\Delta$ , *vide infra*) of 15–30°.<sup>(27)</sup> With its shorter axial bonds and small  $\Delta$  value (10–15°), classification of **2** as a distorted square pyramid, rather than 4 + 1, is more appropriate.

The bichloride-bridged chains form parallel to the *b*-axis (Figure 4a). The nearest interchain chloride–chloride contact distance is 6.853(1) Å (parallel to the *c*-axis). Therefore, the chains are well isolated from each other. The chains form layers in the *bc*-plane (Figure 4b,c). The layers stack parallel to the *a*-axis and are offset with pyridine rings projecting into the space between the layers, thereby minimizing the void volume in the crystal.

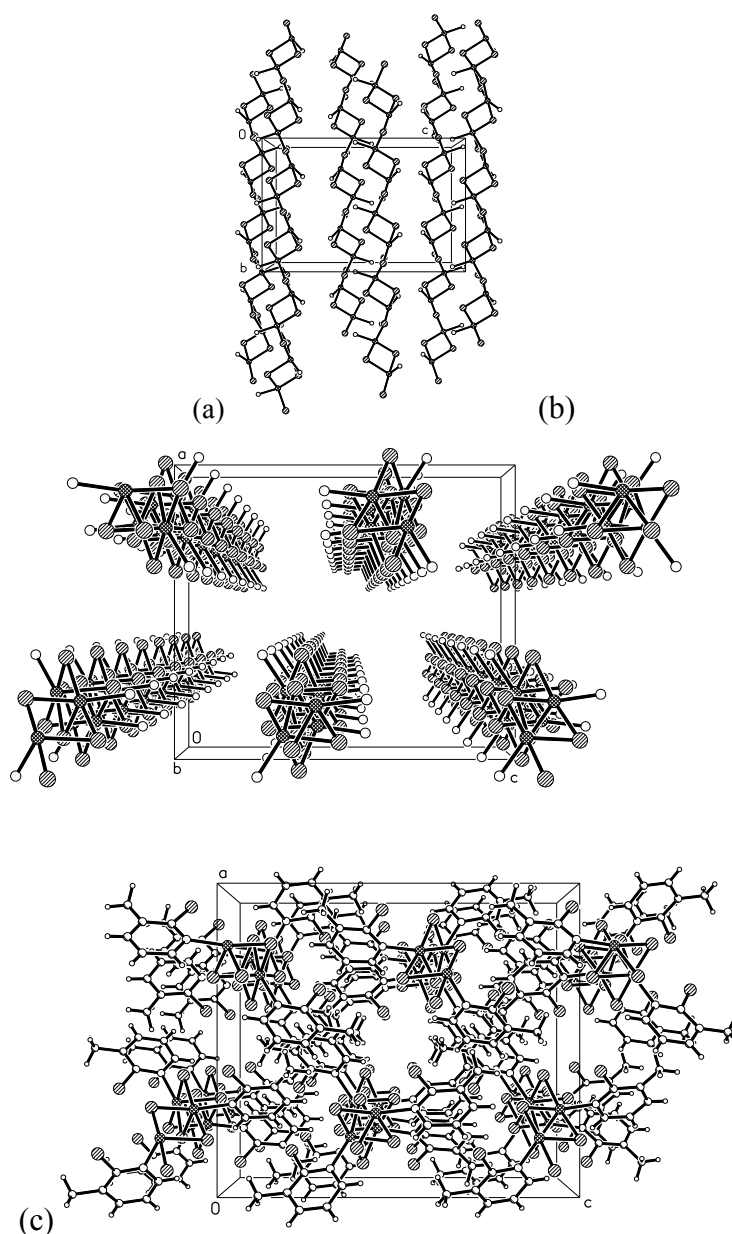


Figure 4: Packing of **2** viewed parallel to the *a*-axis (a) and parallel to the *b*-axis (b and c). Only the copper coordination spheres are shown in (a) and (b) for clarity. (c) Packing diagram viewed parallel to the *b*-axis showing the positions of the pyridine ligands which separate the chains.

### X-ray Structure of *catena*-(2-Bromo-3-methylpyridine)dichlorocopper(II) (**3**)

The asymmetric unit of compound **3** is shown in Figure 5 (selected bond lengths and angles are given in Table 2). Compound **3** crystallizes in the orthorhombic space group *Pbca* and is isomorphous to **2**. Again, there are two crystallographically independent copper ions within the asymmetric unit, both of which are five-coordinate. Bond lengths and angles within the pyridine rings are comparable to those found in **1** and **2** and as

reported for related compounds.<sup>(17)</sup> The pyridine rings are nearly planar with a mean deviation of the constituent atoms of 0.0049 and 0.0041 Å for the N1 and N11 rings, respectively. The bromine and methyl substituents are almost coplanar with the pyridine rings, deviating 0.0183/−0.0126 Å and 0.0069/0.0337 Å, respectively, for the N1 and N11 rings. Each of the pyridine rings occupies an equatorial position of their respective copper coordination spheres.

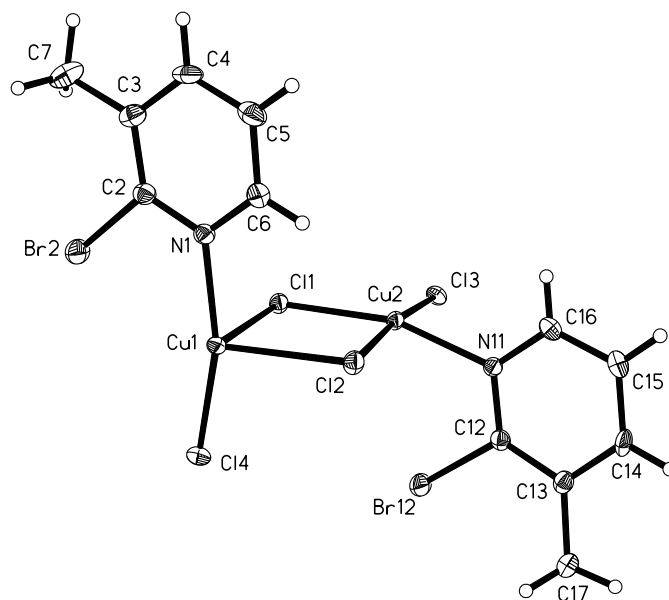


Figure 5: The asymmetric unit of **3** showing 50% probability ellipsoids for refined atoms. Only those atoms whose positions were refined are labeled.

The five-coordinate copper(II) chains of **3** form parallel to the *b*-axis in the same fashion as for **2** (see Figure 3). The CSM approach shows that the two copper coordination spheres are again significantly closer to square pyramidal [ $S(C_{4v}) = 0.902$  and  $1.02$ ] than trigonal bipyramidal, [ $S(D_{3h}) = 3.81$  and  $4.45$ ] for each Cu1 and Cu2, respectively.<sup>(26)</sup> There are eight independent Cu–Cl bonds, which vary in length from 2.2723(9) Å to 2.5712(8) Å. The Cu1–Cl–Cu2 angles range from 89.95(3)° to 95.54(3)°. Similar to **2**, classification as a distorted square pyramid, and not a 4 + 1 geometry, is justified by a short axial bond of 2.5712(8) Å and small  $\Delta$  values of 14.2° (Cu1) and 10.3° (Cu2). Table 3 lists the Cu–Cl bond lengths and bridging angles pertinent to the bibriged chain for **2** and **3**. Similar to **2**, there exist two types of bridges between the copper ions: (1) equatorial–equatorial bridges (Cl1 and Cl3) and (2) axial–equatorial bridges (Cl4 and Cl2). The dihedral angle Cu1–Cl4–Cu2a–Cl2a is −172.3° while that of Cu2a–Cl4–Cu1–Cl2 is 94.0°.

Table 3. Cu–Cl Bond Lengths and Bridging Angles, Cu–Cl–Cu, of the Bi-Bridged Chains Found in **2** and **3**

	length (Å)		length (Å)		angle (deg)
		<b>2</b>			
Cu1–Cl1	2.3400(4)	Cu2A–Cl1	2.3102(4)	Cu–Cl1–Cu	95.399(15)
Cu1–Cl2	2.5581(4)	Cu2A–Cl2	2.2915(4)	Cu–Cl2–Cu	90.171(15)
Cu1–Cl3	2.3196(4)	Cu2A–Cl3	2.3511(4)	Cu–Cl3–Cu	95.177(16)
Cu1–Cl4A	2.2698(4)	Cu2A–Cl4A	2.5524(4)	Cu–Cl4A–Cu	91.114(15)
		<b>3</b>			
Cu1–Cl1	2.3411(8)	Cu2A–Cl1	2.3108(8)	Cu–Cl1–Cu	95.54(3)
Cu1–Cl2	2.5712(8)	Cu2A–Cl2	2.2942(8)	Cu–Cl2–Cu	89.95(3)
Cu1–Cl3	2.3234(8)	Cu2A–Cl3	2.3494(8)	Cu–Cl3–Cu	95.45(3)
Cu1–Cl4A	2.2723(9)	Cu2A–Cl4A	2.5652(9)	Cu–Cl4A–Cu	91.04(3)

The bibridged chains form parallel to the *b*-axis. The nearest interchain chloride–chloride contact distance is 6.875 Å (nearly parallel to the *c*-axis), so again the chains are well isolated. Similar to **2**, the chains of **3** form layers in the *bc*-plane (Figure 4b). The layers stack along the *a*-axis and are offset by the substituted pyridine ligands projecting into the space between the layers.

#### X-ray Structure of *catena*-(2-Chloro-3-methylpyridine)dichlorocopper(II) (**1**)<sup>(28)</sup>

The asymmetric unit of compound **1** is shown in Figure 6. Unlike **2** and **3**, compound **1** crystallizes in the monoclinic space group *C2/c*. Bond lengths and angles of the pyridine ring are comparable to those found in **2** and **3**. The pyridine ring is nearly planar with a mean deviation of the constituent atoms of 0.0452 Å. The chlorine and methyl substituents are nearly coplanar with the mean plane of the pyridine ring, deviating 0.0745 and –0.0362 Å, respectively, but are inclined to opposite sides of the pyridine ring plane.

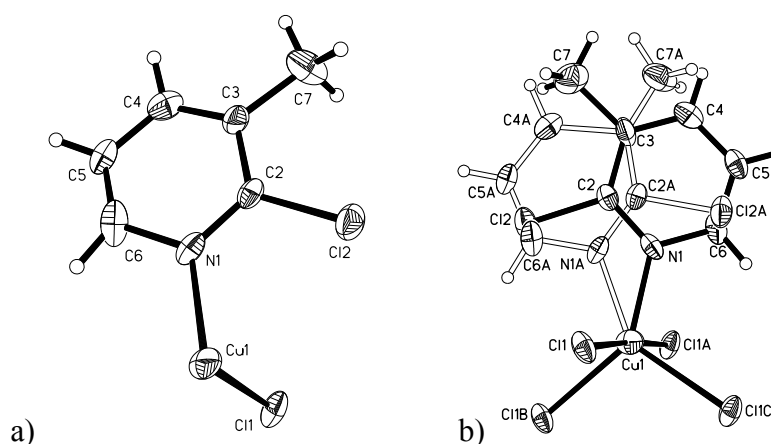


Figure 6: a) The asymmetric unit of **1** showing 50% probability ellipsoids for refined atoms. Hydrogen atoms are not labeled for clarity. b) The Cu coordination sphere in compound **1** including the two sites of the disordered pyridine ligand (N1 ring

has solid bonds while the N1A ring has hollow bonds). Symmetry operators: A, 1-x, y, .5-z; B, 1-x, 1-y, 1-z; C, x, 1-y, z-0.5.

The copper atom sits on a 2-fold axis and thus the pyridine ring is fully disordered with a 50% occupancy for each position as required by symmetry (Figure 6b). There is also only one chloride ion coordinated to the copper ion in the asymmetric unit, which is symmetry generated by the 2-fold axis parallel to the *b*-axis to produce Cl1B. The two additional, coordinated chloride ions are generated by a *c*-glide plane perpendicular to the 2-fold axis.

Compound **1** also forms bi-bridged five-coordinate copper(II) chains (Figure 7). Using the CSM approach,<sup>(22)</sup> the copper coordination sphere is seen to be significantly closer to trigonal bipyramidal [ $S(D_{3h}) = 1.11$ ] than square pyramidal [ $S(C_{4v}) = 3.10$ ]. The geometry of the copper coordination sphere is the same for both disordered sites for the pyridine ligand, as required by symmetry. The copper coordination structure of **1** is similar to that seen in the dimeric anion,  $Cu_2Cl_8^{4-}$ , found in tris(ethylene diamine)cobalt(III) di- $\mu$ -chlorobis-[trichlorocuprate(II)] dichloride dihydrate,  $[Co(en)_3]_2[Cu_2Cl_8]Cl_2 \cdot 2H_2O$ .<sup>(27)</sup> The  $Cu_2Cl_8^{4-}$  anion contains distorted trigonal bipyramidal Cu(II) ions. The distortion of the TBP copper ions in  $Cu_2Cl_8^{4-}$  occurs as an opening of one basal plane angle to  $142.3(2)^\circ$  and the closing of another basal plane angle to  $96.3(2)^\circ$ . The dimer [(2-chloro-3-methylpyridine) $_2CuCl_2$ ] $_2$  exhibits a similar distortion with basal plane angles of  $141.6$ ,  $110.3$ , and  $107^\circ$ .<sup>(17)</sup> The Cu–Cl bond in  $Cu_2Cl_8^{4-}$  that is opposite the large basal plane angle is elongated. This distortion is also found in other five-coordinate copper dimers, such as bis(3-aminopyridinium)hexachloro-dicuprate (II)<sup>(27)</sup> and di- $\mu$ -chlorobis[dichloro(guaninium)copper(II)]dihydrate.<sup>(29)</sup> While the large Cl–Cu–Cl angle is typical of the folded 4 + 1 geometry found in many copper(II) halide salts, the elongated bond is significantly shorter than normal for such species ( $\sim 2.5$  Å vs  $2.7$  Å).

The bond elongation in **1** is observed in the *two* equatorial Cu–Cl bonds with lengths of  $2.458(12)$  Å (Cl1A and Cl1C). Because there is disorder in the position of the pyridine ring, there are two large basal plane angles of  $141.6^\circ$ . Therefore, unlike the reference compounds, and **2** and **3**, which have only one long bond, **1** has two. This long Cu–Cl bond length is intermediate between a typical trigonal bipyramidal terminal ligand ( $2.4$  Å)<sup>(30)</sup> and a square pyramidal terminal ligand ( $2.5$  Å).<sup>(31)</sup>

Blanchette and Willett, working to define a pathway for the transformation from square pyramidal to trigonal bipyramidal, plotted Cu–L' (semicoordinate bond) distances versus the trans angle difference ( $\Delta$ ) of copper(II) chloride complexes.<sup>(27)</sup> They noted that there are only two known compounds which exist geometrically on the conversion line from square pyramidal to trigonal bipyramidal—the 3-aminopyridinium chlorocuprate salt<sup>(27)</sup> and the guaninium dimer.<sup>(30)</sup> Compound **1** also fits this description since it has a Cu–Cl' distance of  $2.458$  Å and a  $\Delta$  value of  $34.4^\circ$ . Table 4 gives a

comparison of bond lengths and angles of **1**, the guaninium dimer, and the 3-aminopyridinium salt.

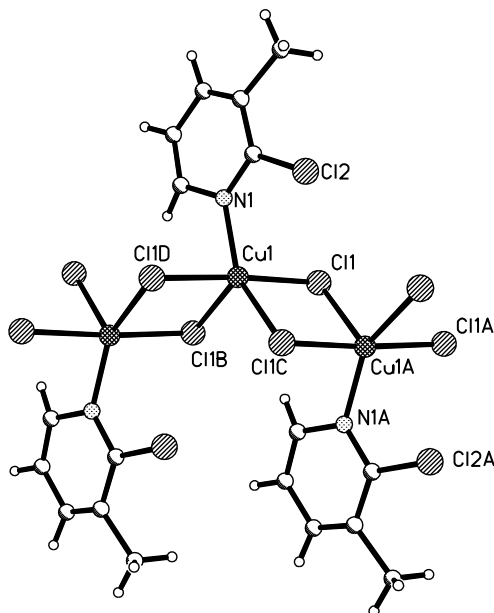


Figure 7: The 5-coordinate copper chain formed by **1**. Only one position for the disordered pyridine ligand per copper ion is shown for clarity. Symmetry operations: A,  $x, 1-y, z+0.5$ ; B,  $x, 1-y, z-0.5$ ; C,  $1-x, 1-y, 1-z$ ; D,  $1-x, y, 0.5-z$ .

Table 4: Comparison table of bond lengths and angles of **1**, di- $\mu$ -chlorobis[dichloro(guaninium)-copper(II)]dihydrate, and bis(3-aminopyridinium)hexachlorodicuprate (II).

	<b>1</b>	<b>Guaninium dimer</b>	<b>3-aminopyridinium salt</b>
Cu-Cl equatorial (Å)	2.458(12)	2.447	2.496
Cu-Cl axial (Å)	2.2915(10)	2.288	2.279/2.320
Cu-Cl-Cu bridge (°)	93.56(4)	98	94.9
$\Delta$ (°)	34.4	35	29.1

Each bridging chloride ion occupies the equatorial position of one copper ion and the axial position of the subsequent copper ion to which it is bonded. This is similar to the guaninium dimer, but differs from the 3-aminopyridinium salt; in the 3-aminopyridinium salt, each of the bridging chloride ions occupies an equatorial position of both copper ions to which it is coordinated. All of the Cu-Cl-Cu bridging angles in **1** are  $93.56(4)^\circ$ , which is smaller than that observed in both the 3-aminopyridinium salt ( $94.9^\circ$ )<sup>(27)</sup> and guaninium dimer ( $98^\circ$ ).<sup>(30)</sup> Compound **1** also differs from the reference

compounds in that the nitrogen containing ligand coordinates to the copper in an equatorial position in place of a fifth chloride ion.

### Magnetic Data

Temperature dependent magnetic data were collected on **2** and **3** from 1.8–310 K. All data were interpreted with the  $H = -\mathcal{J}\sum S_i \cdot S_j$  Hamiltonian. The data [ $\chi T(T)$  and  $1/\chi(T)$ ] for **2** are shown in Figure 8, while those for **3** are shown in Figure 9.

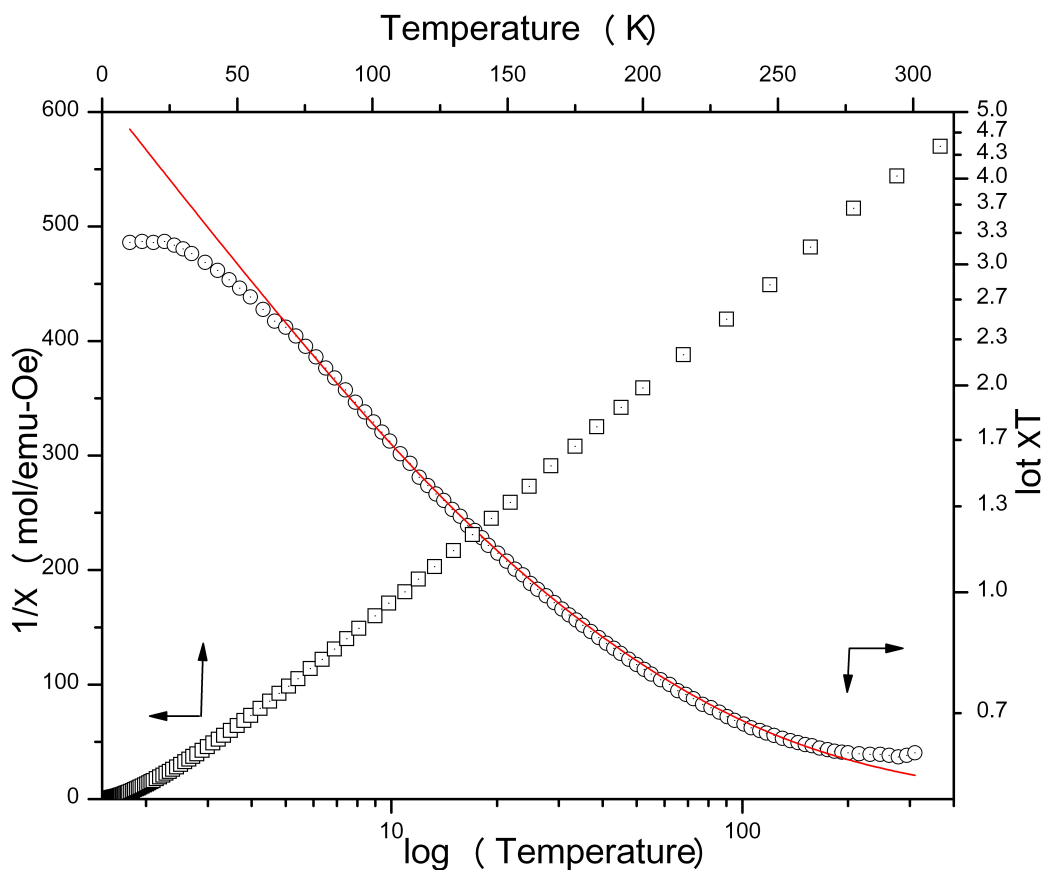


Figure 8. A plot of  $\chi T$  versus  $\log T$  and  $1/\chi$  versus  $T$  for **2**. The solid line shows the fit to a 1D ferromagnetic chain model.

There is no maximum observed in  $\chi(T)$  down to 1.8 K, and the  $\chi T$  product increases sharply with decreasing temperature signifying ferromagnetic interactions. Unlike **1**, no maximum is observed in the plots of  $\chi T(T)$  for either **2** or **3**. The  $\chi_{\text{mol}}$  versus  $T$  data for compounds **2** and **3** were fit with a 1D ferromagnetic chain model.<sup>(32)</sup> At the lowest temperatures (<6 K) the data deviate from the fitted values suggesting weak interchain interactions. X-band EPR spectra were collected at room temperature, yielding  $g_{\parallel} = 2.16$  and a  $g_{\perp} = 2.21$  for **2** and  $g = 2.16$  (isotropic) for **3**. The results of the fitting are presented in Table 5.



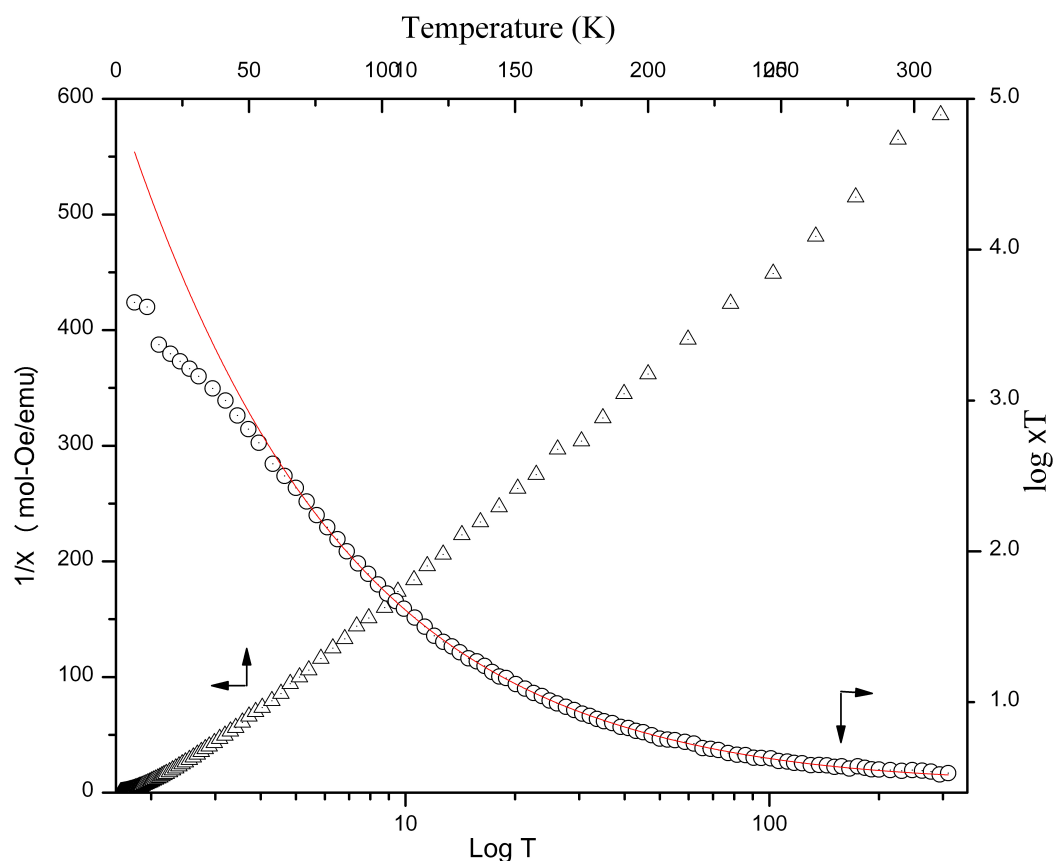


Figure 9. A plot of  $\chi T$  versus  $\log T$  and  $1/\chi$  versus  $T$  for **3**. The solid line shows the fit to a 1D ferromagnetic chain model.

Table 5: Magnetic fitting results for compounds **2** and **3**.

Compound	J (K)	Curie Constant	% error <sup>a</sup>	R <sup>2</sup>
<b>2</b>	69.0(7)	0.487(2)	5.9%	0.99931
<b>3</b>	73.9(4)	0.463(1)	6.3%	0.99977

<sup>a</sup> Difference between fitted value of the Curie constant and that measured by EPR.

### Theoretical Calculations

The model system chosen to carry out this study is shown in Figure 10a. In the chosen model, four consecutive Cu(II) ions were excised from the chain structure; the central Cu–Cu pair has the same chemical environment as is found in the crystal. The segment was terminated by replacing two lateral Cu(II) ions with Zn(II) ions to decrease the complexity of the calculations; the Zn(II) ions have no unpaired electrons and thus do not contribute a magnetic moment, while they mimic quite effectively the electric field generated by the Cu(II) ions which they replace. Two K ions at the end points of the chain have been included to maintain the electroneutrality of the overall system. The pyridine ligands have been replaced by ammonia molecules on the Zn(II) ions to simplify the calculations.

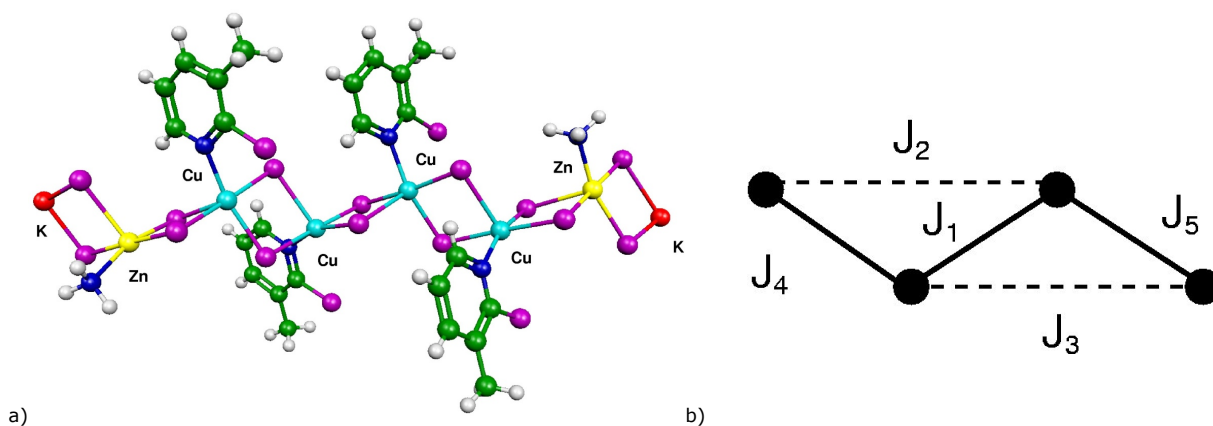


Figure 10. a) Model system used to evaluate magnetic exchange in **2** and **3**. b) Magnetic topology applied to compounds **2** and **3**.  $J_1$  refers to the nearest-neighbor (NN) magnetic interaction of the central Cu—Cu pair.  $J_2$  and  $J_3$  are associated with the magnetic interaction between next-nearest-neighbor Cu<sup>II</sup> ions.  $J_4$  and  $J_5$  refer to NN magnetic interactions between the terminal Cu<sup>II</sup> ion pairs.

The magnetic topology associated with the selected model is schematized in Figure 10b. As shown in this figure, our model systems allow us to evaluate not only the magnetic interactions between nearest-neighbor Cu(II) ions ( $J_1$ ,  $J_4$ , and  $J_5$  in Figure 10b), but also the presence, or absence, of next-nearest-neighbor interactions between Cu(II) ions ( $J_2$  and  $J_3$  in Figure 10b).

The computed  $J$  values are collected in Table 6. All the exchange constants are ferromagnetic for compounds **2** and **3**, including the NNN-exchange between nonadjacent Cu ions (although these NNN-exchange values for **2** and **3** may be considered negligible). The values for **1** have also been included in Table 6 for comparison, and it is worth emphasizing that while the NN-interactions in **1** are also ferromagnetic, the NNN-interactions in **1** are all antiferromagnetic and significantly larger than the values obtained in **2** and **3**. The values presented in Table 6 are in good agreement with those obtained from fitted of the susceptibility as a function of temperature data.

Table 6. Calculated exchange constants for **1-3** (K). See Figure 10 for the definitions of the different  $J$  values.

Compound	$J_1$	$J_2$	$J_3$	$J_4$	$J_5$
<b>2</b>	<b>81.3</b>	<b>0.66</b>	<b>1.45</b>	<b>77.9</b>	<b>81.0</b>
<b>3</b>	<b>80.5</b>	<b>0.66</b>	<b>1.38</b>	<b>77.7</b>	<b>80.1</b>
<b>1<sup>a</sup></b>	<b>49</b>	<b>-12.7</b>	<b>-12.7</b>	<b>49</b>	<b>49</b>

A See Figure 10 for the definitions of the different  $J$  values. The disorder in **1**

leads to three different NN- and NNN-exchange values. The average values are reported for comparison.

## Discussion

A number of penta-coordinate chloride bridged copper chains exhibit ferromagnetic behavior. This family of compounds includes *catena*-(piperazinedium hexachlorodicuprate),<sup>(33)</sup> polymorphs of *catena*-(bis(dimethylammonium)hexachlorodicuprate),<sup>(34)</sup> *catena*-((cyclopentylammonium)trichlorocuprate),<sup>(35)</sup> *catena*-((ethanolammonium)hexachlorodicuprate),<sup>(36)</sup> *catena*-((isopropylammonium)hexachlorodicuprate),<sup>(37)</sup> *catena*-(bis(2-amino-4-chloro-6-methylpyrimidinium)-hexachlorodicuprate),<sup>(38)</sup> *catena*-(tetramethylethylenediiium)hexachlorodicuprate,<sup>(39)</sup> and *catena*-(bis(pyrrolidinium)hexachlorodicuprate).<sup>(40)</sup> The strength and sign of the NN magnetic exchange in these compounds has been tied to two structural parameters: the Cu–Cl–Cu bridging angle ( $\phi$ ) and the bifold angle ( $\sigma$ ) at each Cu-center.<sup>(41)</sup>

It is convenient to think of the chains as a series of bihalide-bridged dimers. A common way of describing distorted square pyramidal copper dimers ( $\text{Cu}_2\text{Cl}_6^{2-}$ ) is through the bifold angle ( $\sigma$ )—the angle between the bridging  $\text{Cu}_2\text{Cl}_2$  plane and the terminal  $\text{CuCl}_3$  plane (the bending of the square pyramidal basal plane). Species with symmetric bridges ( $\phi \approx 96^\circ$ ) and bifold angles,  $\sigma$ , less than  $\sim 25^\circ$  often exhibit antiferromagnetic behavior while species with  $\sigma > \sim 25^\circ$  tend to exhibit ferromagnetic behavior. In **2** and **3**, the axial ligands of Cu1 and Cu2 are involved in the bihalide bridge, and thus the bridging between the centers is not symmetric. This is not often the case in such copper dimers. Axial ligands are more often involved in interdimer interactions, if they are involved at all. The  $\sigma$  values determined for **2** and **3** are well below this  $25^\circ$  threshold, but both compounds exhibit strongly ferromagnetic interactions. The bifold angle was determined by measuring the angle between the  $\text{Cu}_2\text{Cl}_2$  bridging plane and the plane of the Cu, N, and Cl of the opposite side of the basal plane for each copper ion. The bifold angles of **2** are  $14.2^\circ$  for Cu1 and  $18.7^\circ$  for Cu2, while in **3** they are  $14.9^\circ$  for Cu1 and  $18.8^\circ$  for Cu2. It appears that since the bridging between the copper centers is not symmetric, the use of the bifold angle does not adequately classify the magnetic interactions.

While there are many distorted/bifolded square pyramidal copper(II) structures,<sup>(5, 32, 42)</sup> only three structures were found to contain di- $\mu$ -chlorobridged species that had both equatorial–equatorial and axial–equatorial bridges between Cu(II) ions, as seen in **2** and **3**—tetrakis(ethyltrimethylammonium) tetradecachloropentacuprate (II)  $[(\text{ETrMA})_4\text{Cu}_5\text{Cl}_{14}]$ ,<sup>(8)</sup> copper(II) chloride tetramethylenesulfoxide  $[\text{CuCl}_2(\text{TMSO})]$ , and copper(II) chloride dimethyl sulfoxide  $[\text{CuCl}_2(\text{DMSO})]$ .<sup>(12)</sup> While  $\text{CuCl}_2(\text{TMSO})$  and  $\text{CuCl}_2(\text{DMSO})$  are reported to be bridged by two chloride ions and one oxygen atom, the Cu–O distances are quite long ( $\sim 2.9$  Å). Similarly,  $(\text{ETrMA})_4\text{Cu}_5\text{Cl}_{14}$  has

been reported to be tribridged, but with one Cu–Cl distance of over 2.9 Å, which is substantially longer than the other Cu–Cl distances. These longer bridges have been ignored for the current discussion. Unlike **2** and **3**, the Cu–Cl–Cu bridging angles observed in these three compounds are all acute (Table 7). The equatorial-equatorial Cu–Cl bond lengths are normal at ~2.3 Å. The axial Cu–Cl bonds are shorter in **2** and **3** than in the reference compounds by at least 0.1 Å.

Table 7: Comparison of Bond Lengths and Bridging Angles of **2**, **3**, and Reference Compounds CuCl<sub>2</sub>(TMSO),<sup>(12)</sup> CuCl<sub>2</sub>(DMSO),<sup>(12)</sup> and (ETrMA)<sub>4</sub>Cu<sub>5</sub>Cl<sub>14</sub><sup>(8)</sup>

	<b>2</b> (Cu1/Cu2)	<b>3</b> (Cu1/Cu2)	TMSO	DMSO	ETrMA
Eq-eq Cu-Cl (Å)	2.340/2.310 2.351/2.320	2.341/2.311 2.349/2.323	2.321/2.356	2.236/2.352	2.31/2.368 2.34/2.292
Eq-eq Cu-Cl-Cu (°)	95.4 95.2	95.5 95.5	86.7	87.57	84 85
Eq-axial Cu-Cl (Å)	2.292/2.558 2.270/2.552	2.294/2.571 2.272/2.565	2.254/2.663	2.326/2.714	2.308/2.69 2.308/2.60
Eq-axial Cu-Cl-Cu (°)	90.2 91.1	90.0 91.0	81.0	80.92	77.2 79.2
T at $\chi T_{\text{mas}}$	~2 K	~2 K	7.4 K	12.3 K	30 K
Maximum in $\chi$	None	None	3.9 K	5.4 K	~7 K
J (K)	69.0(7)	73.9(4)	78	90	75.4; -2.96

While it has been demonstrated experimentally that hydroxy and alkoxy bridged systems have a direct correlation between the bridging angle,  $\phi$ , and the sign and magnitude of the magnetic exchange,  $J$ , such correlations have not been exhibited by chloro-bridged systems.<sup>(43)</sup> It has been suggested that since the hydroxy and alkoxy bridged systems exhibit regular Cu–O bonds and chloro-bridged systems vary significantly in the Cu–Cl length, the bridging length as well as the bridging Cu–Cl–Cu angle must be taken into consideration. Hatfield and co-workers<sup>(44)</sup> have suggested that the singlet–triplet exchange coupling,  $J$ , varies as a function of the ratio  $\phi/R$ , where  $\phi$  is the Cu–Cl–Cu' bridging angle and  $R$  is the length of the long, out-of-plane Cu–Cl bond. For values of the ratio between 32.6 and 34.8°/Å, the exchange interaction is ferromagnetic. The exchange interaction is antiferromagnetic for ratios below 32.6 and above 34.8°Å<sup>-1</sup>. However, more recent work shows a dependence on the geometry of the copper coordination sphere, i.e., square pyramidal (SP), tetragonal square pyramidal (SPTH), and trigonal bipyramidal (TBP).<sup>(45)</sup> Rojo et al. demonstrated this dependence by plotting  $J$  versus the  $\phi/R$  ratio of a variety of bibringed copper chloride dimers; by connecting the various ratios for SP and SPTH, they show ferromagnetic interactions occurring between 32 and 32.5° for SP and between 32.5 and 34.8° for SPTH. This significantly limits the range at which ferromagnetic interactions are likely to occur. It

is important to recognize that this has been utilized for  $\mu$ -chloride-bridged dimers with axial–equatorial connections.

Isomorphous compounds **2** and **3** have one axial–equatorial and one equatorial–equatorial bridge between each pair of copper ions; there is no inversion center at the bridging center and the bridges are unsymmetrical. There are four independent bridging chloride ions in each compound—two located in ax–eq positions (Cl2 and Cl4) and two in eq–eq positions (Cl1 and Cl3). Therefore, the  $\phi/R$  ratio was calculated for each bridging halide using the long Cu–Cl\* bond and the bridging angle for that particular chloride ion (Table 8). The  $\phi/R$  ratio of the eq–eq bridges is  $\sim 40.7^\circ/\text{\AA}$  for both compounds; this is well outside the limits presented above. The  $\phi/R$  ratio of the ax–eq bridges is between 35 and  $35.7^\circ/\text{\AA}$ . While this lies just outside the limits for the observed ferromagnetic behavior, it would be expected that systems with  $\phi/R$  ratios near the limit values would exhibit weak magnetic interactions. Compounds **2** and **3** exhibit strong ferromagnetic interactions with exchange constants of 69.0(7) K and 73.9(4) K, respectively.

Table 8: Calculations of  $\phi/R$  for **2** and **3** using long Cu–Cl bond length and the respective Cu–Cl–Cu angle. Cl1 and Cl3 form equatorial–equatorial bridges, while Cl2 and Cl4 form axial–equatorial bridges.

<b>2</b>	<b>Cu–Cl* long (Å)</b>	<b>Cu–Cl*–Cu (°)</b>	<b><math>\phi/R</math> (<math>^\circ/\text{\AA}</math>)</b>
Cl1	2.3400(4)	95.399(15)	40.8
Cl2	2.5581(4)	90.171(15)	35.3
Cl3	2.3511(4)	95.177(16)	40.5
Cl4	2.5524(4)	91.114(15)	35.7
<b>3</b>	<b>Cu–Cl* long (Å)</b>	<b>Cu–Cl*–Cu (°)</b>	<b><math>\phi/R</math> (<math>^\circ/\text{\AA}</math>)</b>
Cl1	2.3411(8)	95.54(3)	40.8
Cl2	2.5712(8)	89.95(3)	35
Cl3	2.3494(8)	95.45(3)	40.6
Cl4	2.5652(8)	91.04(3)	35.5

As mentioned previously, reference compounds  $\text{CuCl}_2(\text{TMSO})$ ,  $\text{CuCl}_2(\text{DMSO})$ , and  $(\text{ETrMA})_4\text{Cu}_5\text{Cl}_{14}$  have acute bridging angles; the compounds have comparable Cu–Cl<sub>eq–eq</sub> bond lengths and long Cu–Cl<sub>ax–eq</sub> bond lengths.<sup>(12)</sup> As such, the  $\phi/R$  ratios for  $\text{CuCl}_2(\text{TMSO})$ ,  $\text{CuCl}_2(\text{DMSO})$ , and  $(\text{ETrMA})_4\text{Cu}_5\text{Cl}_{14}$  are smaller than that observed in **2** and **3**. However, the ratios are also not within the limits expected for ferromagnetic material (Table 9). It is clear that the correlation of  $J$  to the  $\phi/R$  ratio may not be employed in the case of eq–eq bridged systems, nor may it be utilized when there is one eq–eq bridge and one ax–eq bridge.

Table 9: A comparison of calculated  $\phi/R$  values for **2**, **3**, and reference compounds  $\text{CuCl}_2(\text{TMSO})$ ,  $\text{CuCl}_2(\text{DMSO})$ , and  $(\text{ETrMA})_4\text{Cu}_5\text{Cl}_{14}$ .

	<b>2</b>	<b>3</b>	<b>TMSO</b>	<b>DMSO</b>	<b>ETrMA</b>
$\phi/R$ ( $^\circ/\text{\AA}$ ) ax-eq	35.3 and 35.7	35 and 35.5	30.4	29.8	28.7 and 30.5
$\phi/R$ ( $^\circ/\text{\AA}$ ) eq-eq	40.8 and 40.5	40.8 and 40.7	36.8	37.2	36.4 and 36.3

The reference compounds  $\text{CuCl}_2(\text{TMSO})$  and  $\text{CuCl}_2(\text{DMSO})$ , as well as  $[(\text{ETrMA})_4\text{Cu}_5\text{Cl}_{14}]$  remain the best basis for comparison of magnetostructural correlations for **2** and **3**. Unlike many of the previously reported chloride bridged systems, these compounds have one ax–eq bridge and one eq–eq bridge, and they behave in comparable ways magnetically (Table 7). Unlike the ETrMA salt, in which the  $\chi T$  product increases to a maximum of 2.8 emu/(K\*mol) at 30 K and then decreases monotonically to zero as the temperature decreases further, the  $\chi T$  product of **2** appears to level off at approximately 2 K and 3.3 emu/(K\*mol); compound **3** behaves similarly. This maximum in the  $\chi T$  product is also observed in  $\text{CuCl}_2(\text{TMSO})$  (at 7.4 K) and  $\text{CuCl}_2(\text{DMSO})$  (at 12.3 K). The reference compounds also reach a maximum in susceptibility,  $\chi$ , but **2** and **3** do not. The fact that there is no observed maximum in susceptibility for **2** and **3**, and the  $\chi T$  product is only leveling off at  $\sim 2$  K indicates a much weaker interchain interaction than that observed in the TMSO, DMSO, and ETrMA complexes which must be antiferromagnetic. This belief is confirmed by the crystal structure which shows that chains of **2** and **3** are well isolated with the closest interchain chloride–chloride contact distance being greater than 6 Å. While compounds **2** and **3** have similar Cu–Cl<sub>eq</sub> bond lengths to TMSO, DMSO, and ETrMA near 2.3 Å, the Cu–Cl<sub>ax</sub> bond lengths are at least a tenth of an angstrom shorter. Compounds **2** and **3** also have slightly obtuse bridging angles, while TMSO, DMSO, and ETrMA have acute bridging angles. The exchange constants for **2** and **3** are comparable to those observed in the TMSO and ETrMA compounds.

The behavior of compound **1** is distinctly different, not solely in terms of the randomness introduced by the crystallographic disorder, but also due to the difference in geometry at the Cu(II) ion and the NNN-exchange which is both stronger and antiferromagnetic. The question of why the position of the pyridine ligand should affect the magnitude of the ferromagnetic exchange between the Cu(II) ions in **1** remains, but the observation that *syn*-orientations lead to larger exchange provides a significant clue. (We define the *syn*-orientation as that where the substituents on the pyridine ring are oriented on the side of the Cu···Cu pair in question, while the *anti*-orientation is that where the substituents are directed away from the Cu···Cu pair in question.) Consider a portion of the chain (Figure 11) and the locations of the pyridine ligands with respect to a pair of adjacent copper ions. Although the structures are slightly better described as trigonal bipyramidal, they are intermediate in nature and the orientation of the metal d-orbitals is highly dependent upon the position of the pyridine ligand. This becomes clear if we examine the Cu1–Cu1A pair (Figure 11).

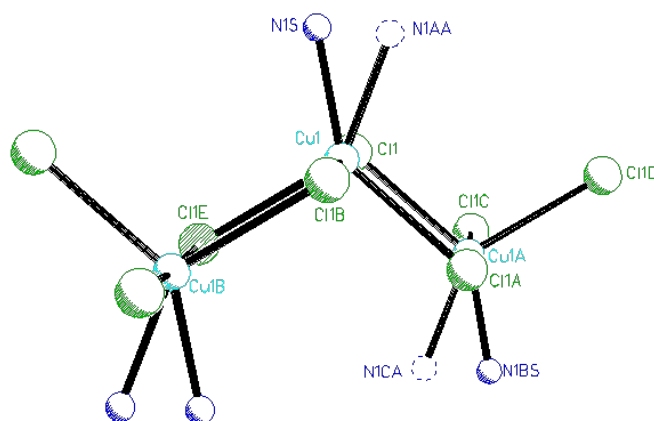
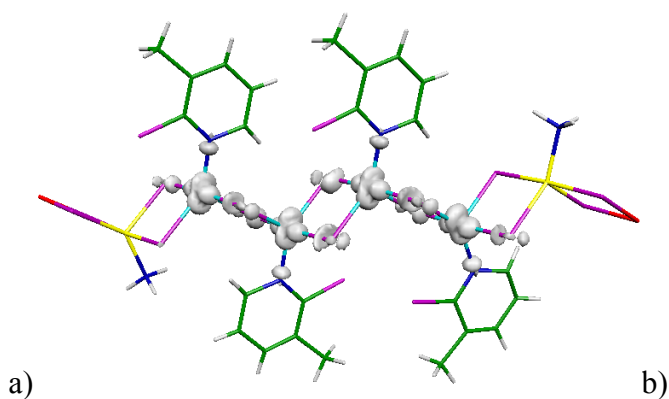


Figure 11 – A portion of the bichloride bridged chain structure of **1**. Only the Cu-coordination spheres are shown for clarity. The atoms N1S and N1BS represent the *syn*-orientation of the pyridine ligands while the atoms N1AA and N1CA (dotted circles) represent the *anti*-orientation with respect to the Cu1-Cu1A pair.

Cu1, Cl1, Cu1A, and Cl1A comprise the planar bridge which provides the principle superexchange pathway for the pair. Cl1B and Cl1C deviate only slightly ( $\sim 0.12$  Å) from that plane. If we consider that the pyridine moiety on Cu1 is in position N1S (the *syn*-position), then we can choose to describe the Cu1 ion as a highly distorted square pyramid with Cl1, Cl1A, Cl1B, and N1S comprising the basal plane (the angles N1A–Cu1–Cl1A and Cl1–Cu1–Cl1B are  $141.6^\circ$  and  $176.0^\circ$ , respectively), and they thence have the greatest overlap with the  $d(x^2 - y^2)$  orbital, while Cl1E is left in the pseudoaxial position. Given this geometry, it is reasonable to assume that the greatest unpaired electron density lies in the  $d(x^2 - y^2)$  orbital and is therefore most delocalized onto these ligands—specifically Cl1 and Cl1A which bridge to Cu1A—leading to stronger exchange between Cu1 and Cu1A. This is supported by the spin-density displayed in Figure 12a.



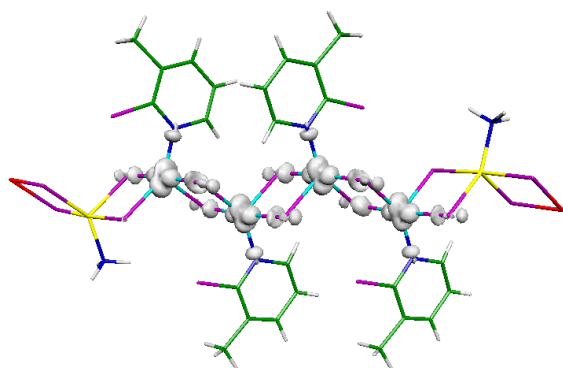


Figure 12. Spin density (cutoff at 0.01) of two different configurations of compound **1**: a *syn*—*syn* configuration for the central pair of Cu ions (*top*), and an *anti*—*anti* configuration for the central pair of Cu ions (*bottom*). These spin densities were obtained from UB3LYP/ TZVP calculations of the high-spin state of the model systems.

The same argument can be made for Cu1A if we take the pyridine to be in the *syn*-position (N1BS) and Cl1, Cl1A, and Cl1C as the other basal ligands. Considered in this fashion, the fold-angle at each Cu1 and Cu1A is 38.9°, much greater than the minimum value of 22° expected for ferromagnetic exchange. If, on the other hand, the pyridine moiety lies in position N1AA (*anti*), then the atoms N1AA, Cl1, Cl1B, and Cl1E would constitute the basal plane and Cl1A would occupy the pseudoaxial position. In this geometry, Cl1 overlaps strongly with the  $d(x^2 - y^2)$  orbital, while Cl1A would overlap more strongly with the  $d(z^2)$ -orbital with its lesser unpaired electron density (see spin density of Figure 12b), leading to weaker exchange. The same arguments are made when the pyridine is in position N1CA on Cu1A. This change in overlap of the bridging chloride ions agrees well with the observed trend of decreasing exchange as the Cu(II) ion pairs migrate from *syn-syn*, to *syn-anti*, to *anti-anti*.

The NNN-exchange occurs via close Cl⋯Cl contacts which are well within the sum of the van der Waals radii for all three compounds. The lack of disorder in the location of the chloride ions in **1** means that the parameters  $d_{\text{Cu-Cl}}$ ,  $d_{\text{Cl}\cdots\text{Cl}}$ ,  $\theta_{\text{Cu-Cl}\cdots\text{Cl}}$ , and  $\theta_{\text{Cl}\cdots\text{Cl-Cu}}$  are unaffected by the position of the pyridine ligand (these parameters have been shown to be significant in the two-halide exchange pathway for bromocuprates).<sup>(46)</sup> The two-halide NNN-superexchange parameters for compounds **1–3** are given in Table 10.

Table 10 – Parameters for two-halide NNN-exchange in compounds **1–3**.<sup>a</sup>

compound	$d_{\text{Cu-Cl}_a}$	$d_{\text{Cu-Cl}_b}$	$d_{\text{Cl}\cdots\text{Cl}}$	$\theta_{\text{Cu-Cl}\cdots\text{Cl}}$	$\theta_{\text{Cl}\cdots\text{Cl-Cu}}$	$\theta_{\text{Cu-Cl}\cdots\text{Cl-Cu}}$
<b>1</b>	2.291	2.458	3.395	135.9	105.3	75.5



<b>2</b> (Cu1···Cu1)	2.340	2.320	3.329	139.8	102.2	96.4
(Cu2···Cu2)	2.310	2.552	3.273	136.7	101.7	81.8
<b>3</b> (Cu1···Cu1)	2.341	2.350	3.334	139.8	101.9	97.5
(Cu2···Cu2)	2.311	2.565	3.277	136.6	101.0	83.2

<sup>a</sup> Note: In compounds **2** and **3** there are two different NNN-pathways due to the presence of two independent Cu(II) ions.

The NNN-superechange pathways for **2** and **3** are virtually identical which agrees well with their isomorphous nature and the calculated values for  $J_{\text{NNN}}$  for the two compounds. The majority of the parameters are also similar when compared to **1**. The Cl···Cl distance is slightly longer in **1**, but there is an interesting difference in Cu–Cl bond lengths. In **2** and **3**, one of the NNN-exchange pathways shows two short Cu–Cl bonds, while the other shows one short and one long Cu–Cl bond. In **1**, all the NNN-pathways are identical, one short and one long Cu–Cl bond, but the long bond is significantly shorter ( $\sim 0.1$  Å) than those of **2** and **3**. The other significant difference lies in the Cu–Cl···Cl–Cu torsion angle. It has been shown in related copper bromide complexes that the superexchange via the two-halide pathway reaches a maximum at values near  $0^\circ$  and  $180^\circ$ , while it approaches zero at torsion angles near  $90^\circ$ . These values are all near  $90^\circ$  for **2** and **3**, while the value for **1** is significantly smaller. Thus, the difference in the sign and magnitude of the NNN-magnetic exchange interactions is not surprising and explains the distinct difference in behavior between **1** and **2/3**.

## Conclusions

The preparation and characterization of the isostructural complexes dichloro(2-chloro-3-methylpyridine)copper(II) (**2**) and isomorphous analogue dichloro(2-bromo-3-methylpyridine)copper(II) (**3**) and their comparison with the known polymorph of **2**, dichloro(2-chloro-3-methylpyridine)copper(II) (**1**) via experimental and computational methods have provided significant magnetostructural information regarding magnetic superexchange in bichloride bridged materials. The very similar structures of **2** and **3**, bichloride bridged chains of five-coordinate Cu(II) ions with a Cl<sub>4</sub>N nearly square-pyramidal coordination sphere, support the observed similarities in their magnetic properties. The magnetic exchange in both compounds is well fitted by a uniform 1D ferromagnetic chain model with negligible next-nearest neighbor and interchain interactions. Comparison to **1**, where the same coordination sphere forms a similar bichloride bridged chain, but where the coordination sphere at each Cu(II) ion is much closer to trigonal bipyramidal, indicates that the difference in geometry is responsible for both a reduction in the nearest neighbor exchange and for the presence of a significant, antiferromagnetic next-nearest neighbor exchange which makes the behavior of **1** very different from **2/3**. Theoretical calculations support both the

magnitude and sign of all fitted exchange values. Further work is in progress to identify additional members of both classes of materials.

### **Acknowledgements**

We thank the Spanish Government for support (Projects MAT2011-25972 and MAT2014-54025-P). We also thank Generalitat de Catalunya (2014SGR1422) and the computer time allocated by CESCO and BSC. J.J.-S. thanks the Departament d'Universitats, Recerca i Societat de la Informació de la Generalitat de Catalunya and the European FP7 Program for the 2010 BP-A 00248 postdoctoral fellowship.

### **Supporting Information**

The crystal structures have been deposited with the CCDC (**2**, #1006829; **3** # 1006829). These data can be obtained free of charge from The Cambridge Crystallographic Data Centre via [www.ccdc.cam.ac.uk/data\\_request/cif](http://www.ccdc.cam.ac.uk/data_request/cif).

## References

- (1) Morosin, B. Structure refinements on dichloro- and dibromobis-(pyridine)copper(II). *Acta Crystallogr., Sect. B: Struct. Crystallogr. Cryst. Chem.* 1975, 31, 632–4.
- (2) (a) Vitorica-Yrezabal, I. J.; Sullivan, R. A.; Purver, S. L.; Curfs, C.; Tang, C. C.; Brammer, L. Synthesis and polymorphism of (4- ClpyH)<sub>2</sub>[CuCl<sub>4</sub>]: solid–gas and solid–solid reactions. *CrystEngComm* 2011, 13, 3189–3196. (b) Shortsleeves, K. C.; Dawe, L. N.; Landee, C. P.; Turnbull, M. M. Transition metal complexes of 2-amino-3,5- dihalopyridines: Synthesis, structures and magnetic properties of Cu(3,5-diCAP)<sub>2</sub> × 2 and Cu(3,5-diBAP)<sub>2</sub> × 2. *Inorg. Chim. Acta* 2009, 362, 1859–66. (c) Chen, X.-D.; Mak, T. C. W. Copper(II) and cadmium(II) complexes of 2-pyridinyl-4-pyridinylmethanone: Supra- molecular architectures consolidated by hydrogen bonding and π–π interaction. *Inorg. Chim. Acta* 2006, 359, 685–9. (d) Awwadi, F. F.; Willett, R. D.; Twamley, B. Tuning Molecular Structures Using Weak Noncovalent Interactions: Theoretical Study and Structure of trans- Bis(2-chloropyridine)dihalocopper(II) and trans-Bis(3- chloropyridine)dibromocopper(II). *Cryst. Growth Des.* 2011, 11, 5316–23. (e) van Albada, G. A.; Tanase, S.; Mutikainen, I.; Turpeinen, U.; Reedijk, J. A bis(chlorido)-bridged linear-chain Cu(II) compound with 7-azaindole as an axial ligand; synthesis, structure, hydrogen bonding and magnetism. *Inorg. Chim. Acta* 2008, 361, 1463–68. (f) Minguez Espallargas, G.; Brammer, L.; van de Streek, J.; Shankland, K.; Florence, A. J.; Adams, H. Reversible Extrusion and Uptake of HCl Molecules by Crystalline Solids Involving Coordination Bond Cleavage and Formation. *J. Am. Chem. Soc.* 2006, 128, 9584–9585. (g) Lah, N.; Leban, I. Three new copper(II) halides with simple pyridine alcohols. *Struct. Chem.* 2010, 21, 263–7. (h) Dubler, E.; Hanggi, G.; Schmalle, H. Crystallographic evidence of preferred N(9)-coordination of xanthine: structures of CuII(xan)<sub>2</sub>(NO<sub>3</sub>)<sub>2</sub>· 2H<sub>2</sub>O, CuII(xan)<sub>2</sub>Cl<sub>2</sub>·2H<sub>2</sub>O, and ZnII(xan)<sub>2</sub>Cl<sub>2</sub> (xan = xanthine). *Inorg. Chem.* 1992, 31, 3728–36. (i) Awwadi, F. F.; Willett, R. D.; Haddad, S. F.; Twamley, B. The Electrostatic Nature of Aryl–Bromine–Halide Synthons: The Role of Aryl–Bromine–Halide Synthons in the Crystal Structures of the trans-Bis(2-bromopyridine)dihalocopper(II) and trans-Bis(3-bromopyridine)dihalocopper(II) Complexes. *Cryst. Growth Des.* 2006, 6, 1833–8. (j) Zhang, W.; Jeitler, J. R.; Turnbull, M. M.; Landee, C. P.; Wei, M.; Willett, R. D. Synthesis, X-ray structures and magnetic properties of linear chain 4-cyanopyridine compounds: [Cu(4-CNpy)<sub>4</sub>(H<sub>2</sub>O)](ClO<sub>4</sub>)<sub>2</sub> and M(4-CNpy)<sub>2</sub>Cl<sub>2</sub> (M = Mn, Fe, Co, Ni, Cu). *Inorg. Chim. Acta* 1997, 256, 183–98.
- (3) (a) Jansen, J. C.; van Koningsveld, H.; van Ooijen, J. A. C. *Cryst. Structure of dibromobis(2-chloroimidazole)copper(II)*. *Struct. Commun.* 1978, 7, 637–41. (b) Estes, W. E.; Gavel, D. P.; Hatfield, W. E.; Hodgson, D. J. Magnetic and structural characterization of dibromo- and dichlorobis(thiazole)copper(II). *Inorg. Chem.* 1978, 17, 1415–21. (c) Prince, B. J.; Turnbull, M. M.; Willett, R. D. Copper(II) Halide Complexes of 2-Aminopyrimidines: Crystal Structures of [(2-aminopyrimidine)<sub>n</sub>CuCl<sub>2</sub>] (n = 1,2) and (2-amino-5- bromopyrimidine)<sub>2</sub>CuBr<sub>2</sub>. *J.*

Coord. Chem. 2003, 56, 441–52. (d) Herringer, S. N.; Longendyke, A. J.; Turnbull, M. M.; Landee, C. P.; Wikaira, J. L.; Jameson, G. B.; Telfer, S. G. Synthesis, structure, and magnetic properties of bis(monosubstituted-pyrazine)- dihalocopper(II). Dalton Trans. 2010, 39, 2785–97. (e) Valle, G.; Ettore, R.; Peruzzo, V. Bis(4-bromopyrazole)dichlorocopper(II). Acta Crystallogr., Sect. C: Cryst. Struct. Commun. 1995, 51, 1293–5.

(4) (a) Helis, H. M.; Goodman, W. H.; Wilson, R. B.; Morgan, J. A.; Hodgson, D. J. A novel halogen-bridged system: synthesis and structures of dibromo[2-(2-aminomethyl)pyridine]copper(II) and dibromo(2-methyl-1,2-diaminopropane)copper(II). Inorg. Chem. 1977, 16, 2412–6. (b) Garland, M. T.; Grandjean, D.; Spodine, E.; Atria, A. M.; Manzur, J. Structure of dibromo(1,10-phenanthroline)- copper(II). Acta Crystallogr., Sect. C: Cryst. Struct. Commun. 1988, 44, 1547–9. (c) Hammond, R. P.; Cavaluzzi, M.; Haushalter, R. C.; Zubieta, J. A. Investigations of the Copper Bromide-2,2'-Dipyridyl System: Hydrothermal Synthesis and Structural Characterization of Molecular  $\text{Cu}_3\text{Br}_4(\text{C}_{10}\text{H}_8\text{N}_2)_2$ , One-Dimensional  $\text{CuBr}_2(\text{C}_{10}\text{H}_8\text{N}_2)$ , and Two-Dimensional  $[\text{Cu}_2(\text{OH})_2(\text{C}_{10}\text{H}_8\text{N}_2)_2] \cdot [\text{Cu}_4\text{Br}_6]$ . Inorg. Chem. 1999, 38, 1288–92. (d) Głowka, M. L.; Galdecki, Z.; Kazimierzczak, W.; Maslinski, C. Structure of the 1:1 complex of histamine with copper(II) chloride. Acta Crystallogr., Sect. B: Struct. Crystallogr. Cryst. Chem. 1980, 36, 2148–2150. (e) Maslak, P.; Szczepanski, J. J.; Parvez, M. Complexation through nitrogen in copper and nickel complexes of substituted ureas. J. Am. Chem. Soc. 1991, 113, 1062–3. (f) Mahmoudi, A.; Khalaj, M.; Gao, S.; Ng, S. W.; Mohammadgholiha, M. Dichlorido{2-[(4-iodophenyl)iminomethyl]pyridine-2N,N'}-copper(II). Acta Crystallogr., Sect. E: Struct. Rep. Online 2009, 65, m555. (g) Canellas, P.; Bauza, A.; Garcia-Raso, A.; Fiol, J. J.; Deya, P. M.; Molins, E.; Mata, I.; Frontera, A. Synthesis, X-ray characterization and computational studies of Cu(II) complexes of N-pyrazolyl pyrimidine. Dalton Trans. 2012, 41, 11161–9.

(5) Battaglia, L. P.; Bonamartini Corradi, A. B.; Marcotrigiano, G.; Menabue, L.; Pellacani, G. C. Spectroscopic and structural investigation on the trihalocuprates(II) of the 4-benzylpiperidinium cation. Crystal and molecular structure of bis(4-benzylpiperidinium) hexachlorodicuprate(II). Inorg. Chem. 1980, 19, 125–129.

(6) Willett, R. D. Crystal Structure and Optical Properties of  $(\text{CH}_3)_2\text{NH}_2\text{CuCl}_3$ . J. Chem. Phys. 1966, 44, 39–42.

(7) Sun, H.; Harms, K.; Sundermeyer, J. The crystal structure of a metal-containing ionic liquid: A new octachlorotricuprate(II). Z. Kristallogr. - Cryst. Mater. 2005, 220, 42–4.

(8) Bond, M. R.; Willett, R. D.; Rubenacker, G. V. Crystal structures and magnetic behavior of two novel copper(II) halide chains.  $(\text{C}_7\text{H}_{10}\text{N})_4\text{Cu}_5\text{Cl}_{14}$  and  $(\text{C}_5\text{H}_{14}\text{N})_4\text{Cu}_5\text{Cl}_{14}$ : multiple copper(II) halide coordination geometries. Inorg. Chem. 1990, 29, 2713–20.

- (9) Fujii, Y.; Wang, Z.; Willett, R. D.; Zhang, W.; Landee, C. P. Crystal Structure of (Et<sub>2</sub>Me<sub>2</sub>N)<sub>3</sub>Cu<sub>4</sub>Cl<sub>11</sub>: An Antiferromagnetic Chain of Ferromagnetically Coupled Tetramers. *Inorg. Chem.* 1995, 34, 2870–4.
- (10) Willett, R. D.; Bond, M. R.; Haije, W. G.; Soonieus, P. M.; Maaskant, W. J. A. Crystal structures of three phases of tetramethylammonium trichlorocuprate(II) (TMCuCl<sub>3</sub>). *Inorg. Chem.* 1988, 27, 614–20.
- (11) Klement, U. Die Kristallstruktur des Dimethylnitrosamin- kupfer(II)-chlorids, (CH<sub>3</sub>)<sub>2</sub>NNO.CuCl<sub>2</sub> *Acta Crystallogr., Sect. B: Struct. Crystallogr. Acta Crystallogr., Sect. B: Struct. Crystallogr. Cryst. Chem.* 1969, 25, 2460–65.
- (12) Swank, D. D.; Landee, C. P.; Willett, R. D. Crystal structure and magnetic susceptibility of copper (II) chloride tetramethylsulfoxide [CuCl<sub>2</sub>(TMSO)] and copper (II) chloride monodimethylsulfoxide [CuCl<sub>2</sub>(DMSO)]: Ferromagnetic spin-1/2 Heisenberg linear chains. *Phys. Rev. B: Condens. Matter Mater. Phys.* 1979, 20, 2154–62.
- (13) Barnes, J. C.; Paton, J. D.; McKissock, A. Structures of two complexes of copper(II) chloride and 1, 4- oxathiane. The two- dimensional polymers poly[di-μ-chloro-μ-(1, 4- oxathiane- O, S) - copper(II) ], [Cu<sub>3</sub>(C<sub>4</sub>H<sub>8</sub>OS)<sub>2</sub>Cl<sub>6</sub>]<sub>n</sub>, and poly[dichlorobis-μ-(1, 4- oxathiane- O, S) - copper(II) ], [Cu(C<sub>4</sub>H<sub>8</sub>OS)<sub>2</sub>Cl<sub>2</sub>]<sub>n</sub>. *Acta Crystallogr., Sect. C: Cryst. Struct. Commun.* 1983, 39, 547–50.
- (14) Lyakhov, A. S.; Gaponik, P. N.; Degtyarik, M. M.; Matulis, V. E.; Matulis, V. E.; Ivashkevich, L. S. catena-Poly[[tetrakis(2-allyltetrazole-? N<sub>4</sub>)-tetra-μ-chloro-tricopper(II)]-di-μ-chloro]. *Acta Crystallogr., Sect. C: Cryst. Struct. Commun.* 2003, 59, m90–2.
- (15) Herringer, S. N.; Deumal, M.; Ribas-Arino, J.; Novoa, J. J.; Landee, C. P.; Wikaira, J. L.; Turnbull, M. M. S = 1/2 One- Dimensional Random-Exchange Ferromagnetic Zigzag Ladder, Which Exhibits Competing Interactions in a Critical Regime. *Chem. - Eur. J.* 2014, 20, 8355–62.
- (16) A preliminary description of the synthesis has appeared in ref 15.
- (17) Herringer, S. N.; Turnbull, M. M.; Landee, C. P.; Wikaira, J. L. Copper(II) complexes of 2-halo-3-methylpyridine: synthesis, structure, and magnetic behaviour of Cu(2-X-3-CH<sub>3</sub>py)<sub>2</sub>X<sub>2</sub> [X, X? = chlorine or bromine; py = pyridine]. *Dalton Trans.* 2011, 40, 4242–52.
- (18) Sheldrick, G. M. SHELXTL: v. 5.10, Structure Determination Software Suite; Bruker AXS Inc.: Madison, WI, 2001.
- (19) Sheldrick, G. M. SADABS. Program for Empirical Absorption Correction of Area Detector Data; University of Göttingen: Germany, 1996.
- (20) Sheldrick, G. M. *Acta Crystallogr., Sect. A: Found. Crystallogr.* 2008, 64, 112.
- (21) Carlin, R. L. *Magnetochemistry*, Springer-Verlag, 1986.

- (22) Frisch, M. J.; Trucks, G. W.; Schlegel, H. B.; Scuseria, G. E.; Robb, M. A.; Cheeseman, J. R.; Scalmani, G.; Barone, V.; Mennucci, B.; Petersson, G. A.; Nakatsuji, H.; Caricato, M.; Li, X.; Hratchian, H. P.; Izmaylov, A. F.; Bloino, J.; Zheng, G.; Sonnenberg, J. L.; Hada, M.; Ehara, M.; Toyota, K.; Fukuda, R.; Hasegawa, J.; Ishida, M.; Nakajima, T.; Honda, Y.; Kitao, O.; Nakai, H.; Vreven, T.; Montgomery, Jr., J. A.; Peralta, J. E.; Ogliaro, F.; Bearpark, M.; Heyd, J. J.; Brothers, E.; Kudin, K. N.; Staroverov, V. N.; Kobayashi, R.; Normand, J.; Raghavachari, K.; Rendell, A.; Burant, J. C.; Iyengar, S. S.; Tomasi, J.; Cossi, M.; Rega, N.; Millam, J. M.; Klene, M.; Knox, J. E.; Cross, J. B.; Bakken, V.; Adamo, C.; Jaramillo, J.; Gomperts, R.; Stratmann, R. E.; Yazyev, O.; Austin, A. J.; Cammi, R.; Pomelli, C.; Ochterski, J. W.; Martin, R. L.; Morokuma, K.; Zakrzewski, V. G.; Voth, G. A.; Salvador, P.; Dannenberg, J. J.; Dapprich, S.; Daniels, A. D.; Farkas, O.; Foresman, J. B.; Ortiz, J. V.; Cioslowski, J.; Fox, D. J. Gaussian 09, Revision B.1; Gaussian, Inc.: Wallingford, CT, 2009.
- (23) Becke, A. D. Density-functional thermochemistry. III. The role of exact exchange. *J. Chem. Phys.* 1993, 98, 5648–52.
- (24) Schäfer, A.; Huber, C.; Ahlrichs, R. Fully optimized contracted Gaussian basis sets of triple zeta valence quality for atoms Li to Kr. *J. Chem. Phys.* 1994, 100, 5829–35.
- (25) Ruiz, E.; Rodríguez-Fortea, A.; Cano, J.; Alvarez, S.; Alemany, P. About the calculation of exchange coupling constants in polynuclear transition metal complexes. *J. Comput. Chem.* 2003, 24, 982–989.
- 26) (a) Pinsky, M.; Avnir, D. Continuous Symmetry Measures. 5. The Classical Polyhedra. *Inorg. Chem.* 1998, 37, 5575–82. (b) Landry, B. R.; Turnbull, M. M.; Twamley, B. Synthesis and structure of a novel copper (II) nitrate complex of 2,4-dioxo-4-phenylbutanoic acid. *J. Chem. Crystallogr.* 2007, 37, 81–86. (c) Alvarez, S.; Alemany, P.; Casanova, C.; Cirera, J.; Llunell, M.; Avnir, D. Shape maps and polyhedral interconversion paths in transition metal chemistry. *Coord. Chem. Rev.* 2005, 249, 1693–1708.
- (27) Blanchette, J. T.; Willett, R. D. Magnetic and structural correlations in [(C<sub>5</sub>H<sub>5</sub>N)NH<sub>2</sub>]<sub>2</sub>Cu<sub>2</sub>Cl<sub>6</sub> and [(C<sub>5</sub>H<sub>5</sub>N)NH<sub>2</sub>]<sub>2</sub>Cu<sub>2</sub>Br<sub>6</sub>•H<sub>2</sub>O. *Inorg. Chem.* 1988, 27, 843–9.
- (28) A preliminary description of the structure has appeared in ref 15.
- (29) (a) Carrabine, J. A.; Sundaralingam, M. Stereochemistry of Nucleic Acids and Their Constituents. VIII. Metal Binding Studies. Crystal Structure of a Guanine-Copper Chloride Complex, a Trigonal-Bipyramidally Coordinated Copper. *J. Am. Chem. Soc.* 1970, 92, 369–71. (b) Drake, R. F.; Crawford, V. H.; Laney, N. W.; Hatfield, W. E. Magnetic properties of di-μ<sub>2</sub>-chlorobis[dichloro(guaninium)copper(II)] dihydrate. Second determination. *Inorg. Chem.* 1974, 13, 1246–49.
- (30) Bertrand, A.; Kelley, J. A. The structure of 2,4-oxo-hexa-2-bromo-tetra[amminecopper(II)]. *Inorg. Chim. Acta* 1970, 4, 526–528.
- (31) Antolini, L.; Marcotrigiano, G.; Menabue, L.; Pellacani, G. C. Spectroscopic and structural investigation on the pentachloro- and (mixed-pentahalo)cuprates(II) of the N-

(2-ammoniummethyl)- piperazinium cation. The first case of monomeric pentahalocuprate(II) having square-pyramidal structure. Crystal and molecular structure of the (N-(2-ammoniummethyl)piperazinium) pentachlorocuprate(II) di- hydrate. *J. Am. Chem. Soc.* 1980, 102, 1303–9.

(32) (a) Takahashi, M. Few-dimensional Heisenberg ferromagnets at low temperature. *Phys. Rev. Lett.* 1987, 58, 168–70. (b) Oitmaa, J.; Bornilla, E. High-temperature-series study of the spin-1/2 Heisenberg ferromagnet. *Phys. Rev. B: Condens. Matter Mater. Phys.* 1996, 53, 14228–35.

(33) (a) Battaglia, L. P.; Corradi, A. B.; Geiser, U.; Willett, R. D.; Motori, A.; Sandrolini, F.; Antolini, L.; Manfredini, T.; Menabue, L.; Pellacani, G. C. The crystal structures, magnetic and electrical properties of two polymeric chlorocuprate(II) compounds. *J. Chem. Soc., Dalton Trans.* 1988, 265–71. (b) Daoud, A.; Ben Salah, A.; Chappert, C.; Renard, J. P.; Cheikhrouhou, A.; Duc, T.; Verdaguer, M. Crystal structure and magnetic properties of piperazinium hexadi- chlorocuprate: A new  $S = (1/2)$  antiferromagnetic chain with alternating exchange. *Phys. Rev. B: Condens. Matter Mater. Phys.* 1986, 33, 6253–6260.

(34) Willett, R. D.; Twamley, B.; Montfrooij, W.; Granroth, G. E.; Nagler, S. E.; Hall, D. W.; Park, J.-H.; Watson, B. C.; Meisel, M. W.; Talham, D. R. Dimethylammonium Trichlorocuprate(II):? Structural Transition, Low-Temperature Crystal Structure, and Unusual Two- Magnetic Chain Structure Dictated by Nonbonding Chloride? Chloride Contacts. *Inorg. Chem.* 2006, 45, 7689–97.

(35) Geiser, U.; Gaura, R. M.; Willett, R. D.; West, D. X. Structure and magnetism in  $ACuCl_3$  salts containing bibriged chains with square-pyramidal coordination geometry. *Inorg. Chem.* 1986, 25, 4203–12.

(36) Scott, B.; Willett, R. D. Structural and magnetic properties of bis(ethanolammonium)hexahalodicuprate(II) salts: Copper(II) halide dimers with a square-pyramidal type distortion. *Inorg. Chim. Acta* 1988, 141, 193.

(37) Roberts, S. A.; Bloomquist, D. R.; Willett, R. D.; Dodgen, H. W. Thermochromic phase transitions in copper(II) halide salts. 1. Crystal structure and magnetic resonance studies of isopropylammonium trichlorocuprate(II). *J. Am. Chem. Soc.* 1981, 103, 2603–10.

(38) Diaz, I.; Fernandez, V.; Belsky, V. K.; Martinez, J. L. Synthesis and Structural Study of the Thermochromic Compounds Bis(2-amino- 4-oxo-6-methylpyrimidinium) Tetrachlorocuprate(II) and Bis(2- amino-4-chloro-6-methylpyrimidinium) Hexachlorodicuprate(II). *Z. Naturforsch., B: J. Chem. Sci.* 1999, 54, 718–724.

(39) Willett, R. D. (N, N, N?, N?-tetramethylethylenediammonium)-  $Cu_2 \times 6$  (X = Cl, Br): crystal structure and magnetic interactions Transition. *Transition Met. Chem.* 1987, 12, 410–13.

(40) Wei, M.; Willett, R. D.; Teske, D.; Subbaraman, K.; Drumheller, J. E. Crystal Structure and Magnetic Susceptibility Study of Pyrrolidinium Trichlorocuprate(II). *Inorg. Chem.* 1996, 35, 5781–5.

(41) (a) O'Brien, S.; Gaura, R. M.; Landee, C. P.; Ramakrishna, B. L.; Willett, R. D. Magneto-structural correlations in chains of bifolded Cu<sub>2</sub>Cl<sub>6</sub>? dimers *Inorg. Chim. Acta* 1988, 141, 83–9. (b) Willett, R. D.; Geiser, U. Structural characteristics of ACuCl<sub>3</sub> salts. *Croat. Chem. Acta* 1984, 57, 737–747.

(42) (a) Willett, R. D. Crystal Structure and Optical Properties of (CH<sub>3</sub>)<sub>2</sub>NH<sub>2</sub>CuCl<sub>3</sub> *J. Chem. Phys.* 1966, 44, 39–42. (b) Watkins, N. T.; Dixon, E. E.; Crawford, V. H.; McGregor, K. T.; Hatfield, W. E. Chloro-bridged triplet ground-state copper(II) dimer. *J. Chem. Soc., Chem. Commun.* 1973, 133–4. (c) DeMunno, G.; Denti, G.; Dapporto, P. Synthesis and characterization of dinuclear copper(II) complexes crystal structure of aquatetrachloro-3, 6-bis(2'-pyridyl)pyridazine-dicopper(II). *Inorg. Chim. Acta* 1983, 74, 199–203. (d) Marsh, W. E.; Hatfield, W. E.; Hodgson, D. J. Synthesis of 4-methylthiazole complexes of copper(II) chloride. Structure of a mixed-valent dimer, CuIICuI(4-Metz)4Cl<sub>3</sub>. *Inorg. Chem.* 1983, 22, 2899–903.

(43) (a) Vasilevsky, I.; Rose, N. R.; Stenkamp, R.; Willett, R. D. Crystal structure and magnetic behavior of (tetramethylcyclotetraaza-tetradecatetraene) copper tetrachlorocuprate: an alternating-metal-site, alternating-exchange, spin 1/2 linear-chain system. *Inorg. Chem.* 1991, 30, 4082–4. (b) Lewis, D. L.; Hatfield, W. E.; Hodgson, D. J. Crystal and molecular structure of di-μ<sub>2</sub>-hydroxo-bis[2-(2-ethylaminoethyl)-pyridine]dicopper(II) perchlorate. *Inorg. Chem.* 1972, 11, 2216–21. (c) Laurent, J.-P.; Bonnet, J.-J.; Nepveu, F.; Astheimer, H.; Walz, L.; Haase, W. Crystal and molecular structure and magnetic properties of a tetrameric copper(II) complex with 3-hydroxy-5-hydroxymethyl-4-(4'-hydroxy-3'-methyl-4'-phenyl-2'-azabut-1'-en-1'-yl)-2-methylpyridine (H<sub>2</sub>L): [Cu<sub>4</sub>L<sub>4</sub>]·8MeOH, a complex with a ferromagnetic ground state. *J. Chem. Soc., Dalton Trans.* 1982, 2433–8. (d) Mikuriya, M.; Okawa, H.; Kida, S. Binuclear metal complexes. XLIV. Crystal structures and magnetic properties of alkoxy-oxygen bridged binuclear copper(II) complexes with 2-[2-(dialkylamino)ethylthio] ethanol *Bull. Chem. Soc. Jpn.* 1982, 55, 1086–91.

(44) (a) Marsh, W. E.; Hatfield, W. E.; Hodgson, D. J. Magnetic interactions in chloro-bridged dimers. Structural characterization of aquadichlorobis(2-methylpyridine)copper(II) and bis[dichlorobis(2-methylpyridine)copper(II)]. *Inorg. Chim. Acta* 1982, 21, 2679–84. (b) Tosik, A.; Maniukiewicz, W.; Bukowska-Strzyzewska, M.; Mrozinski, J.; Sigalas, M. P.; Tsipis, C. A. A new structural type for a binuclear chloride-bridged copper(II) complex. Structural and magnetic characterization of di-μ<sub>2</sub>-chloro-chloropentakis-(benzimidazole) dicopper(II) monochloride tetrahydrate, [Cu<sub>2</sub>Cl<sub>3</sub>(C<sub>7</sub>H<sub>6</sub>N<sub>2</sub>)<sub>5</sub>]Cl·4H<sub>2</sub>O. *Inorg. Chim. Acta* 1991, 190, 193–203. (c) Tuna, F.; Patron, L.; Journaux, Y.; Andruh, M.; Plass, W.; Trombee, J.-C. Synthesis and magnetic properties of a series of bi- and tri-nuclear complexes of copper(II) with the unsymmetrical tetradentate Schiff-base ligand 3-[N-(2-(pyridylethyl)formimidoyl)]-salicylic acid, H<sub>2</sub>f<sub>2</sub>saep, and crystal structures of [Cu(Hf<sub>2</sub>saep)Cl]<sub>2</sub> and [Cu(f<sub>2</sub>saep)(H<sub>2</sub>O)]<sub>2</sub>. *J. Chem. Soc., Dalton Trans.* 1999, 539–546.

(45) Rojo, T.; Arriortua, M. I.; Ruiz, J.; Darriet, J.; Villeneuve, G.; Beltran-Porter, D. Magnetostructural correlations in parallel square-planar chloride bridged copper(II) dimers: structure, dynamic nuclear magnetic resonance study, and magnetic properties of [Cu<sub>2</sub>(terpy)-2Cl<sub>2</sub>][PF<sub>6</sub>]<sub>2</sub>. *J. Chem. Soc., Dalton Trans.* 1987, 285.

(46) Turnbull, M. M.; Landee, C. P.; Wells, B. M. Magnetic exchange interactions in tetrabromocuprate compounds *Coord. Chem. Rev.* 2005, 249, 2567–2576.